Electronic Supplementary Information

Visible light promoted PANI@Au:CuO catalyzed sequential amination, azidation and annulation for the preparation of 2-arylbenzimidazoles

Radhika Chopra, Manoj Kumar,* Neelam, Vandana Bhalla*

Department of Chemistry, UGC-Centre for Advanced Studies, Guru Nanak Dev University, Amritsar, Punjab, India.

Email: vanmanan@yahoo.co.in

Page No. Contents

General experimental methods[1]

"UV-vis spectra were recorded on a SHIMADZU UV-2450 spectrophotometer using a quartz cuvette (path length, 1 cm). The fluorescence spectra were obtained with a SHIMADZU 5301 PC spectrofluorimeter. TEM images were recorded in Transmission Electron Microscope (TEM-JEOL 2100F). X-ray diffraction patterns were collected using Rigaku Xpert Pro-X-ray diffractometer provided with CuKα radiation (1.541 A^0) in the 2θ range of 5-80^{0}C at a step size of 0.02^0. The dynamic light scattering (DLS) data were recorded with MALVERN Instruments (Nano-ZS). Infrared spectra were obtained on Varian 660-IR spectrometer using KBr pellets. X-ray photoelectron spectra (XPS) were acquired in PHI Versa Prob 5000. The amount of Au and Cu in catalyst was determined by atomic absorption spectrophotometer (GBC Avant Ver 1.31). Sample preparation was done by reflux assisted digestion of 2 mg of catalyst with concentrated HNO_3. The resulting solution was cooled, centrifuged and filtered. The filtrate was diluted to 10 times with deionized water. Cyclic Voltammetry studies were performed on CH Instruments CH1660D in presence of supporting electrolyte 0.1 M tetrabutylammonium perchlorate (Bu_4NClO_4), Ag/AgCl as reference electrode, platinum wire as counter electrode and glass carbon electrode as working electrode. TEM and HR-TEM images were recorded using HR-TEM-JEM 2100 microscope. To record FT-IR spectra, VARIAN 660 IR Spectrometer was used. Thermogravimetric analysis (TGA) was carried out on EXSTAR TG/DTA 3600 at a heating rate of 100°C/min under nitrogen atmosphere. Photocatalytic experiments were carried out by using the 100 W tungsten filament bulb as irradiation source. ^{1}H NMR spectra were recorded on a JEOL-FT NMR-AL 400 MHz and Bruker (Avance II) FT-NMR 500 MHz spectrophotometer using DMSO-d_6/$CDCl_3$ as solvents and tetramethylsilane ($Si(CH_3)_4$) for internal standards. Further, NMR data was expressed as follows:

chemical shifts in ppm (δ) and coupling constants in Hz (*J*). Multiplicites of signals were quoted as follows: s = singlet, d = doublet, br s = broad singlet, t = triplet and m = multiplet."

Quantum yield calculations

"To find out the fluorescence quantum yield of derivative **4**, solution of diphenylanthracene (Φ_{fr} = 0.90 in cyclohexane) was used as reference at an excitation wavelength (λ_{ex}) of 310 nm. Further, the following equation was used to determine the quantum yield:

$$\phi_{fs} = \phi_{fr} \times \frac{1\text{-}10^{-ArLr}}{1\text{-}10^{-ArLr}} \times \frac{N_s^2}{N_r^2} \times \frac{D_s}{D_r}$$

Φ_{fs} and Φ_{fr} signify the fluorescence quantum yields of sample and reference, respectively. L_s, A_s, D_s and N_s are the length of the absorption cells, absorbance, respective areas of emission and refractive index of sample, respectively. L_r, A_r, D_r and N_r are the length of the absorption cells, absorbance, respective areas of emission and refractive index of reference, respectively."

EXPERIMENTAL SECTION

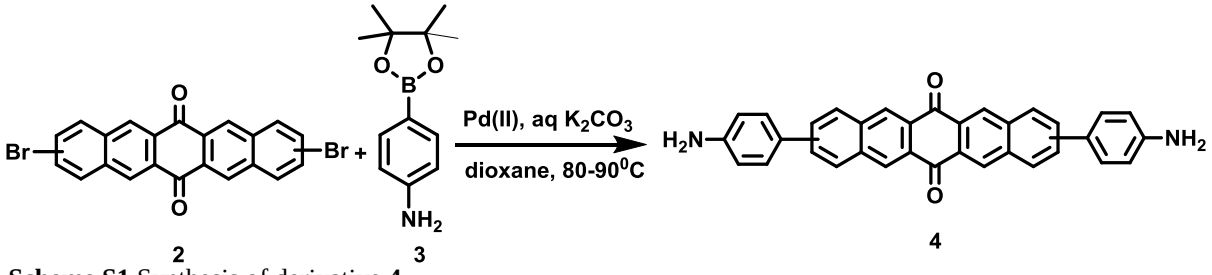

Scheme S1 Synthesis of derivative **4**

To a mixture of compounds **2** (0.5 g, 1.07 mmol) and **3** (0.52 g, 2.36 mmol) in 20 mL of 1,4-dioxane was added 1 mL of aqueous solution of K_2CO_3 (1.1 g, 8.58 mmol) followed by addition of $[Pd(Cl_2)(PPh_3)_2]$ (0.451 g, 0.64 mmol) under N_2 atmosphere (Scheme S1). The reaction mixture was refluxed for 24 h. After completion of the reaction, the excess solvent was removed under reduced pressure and the residue so obtained was dissolved in DCM. The organic layer was washed with water, dried over anhydrous Na_2SO_4, and removed under reduced pressure to give a crude product which was purified by column chromatography using chloroform/methanol (95:5) as an eluent to afford derivative **4** as orange solid (0.294 g in 56% yield); mp: >280 °C. ^{1}H NMR

(400 MHz, $CDCl_3$, ppm) δ = 8.94 (s, 2H), 8.93 (s, 2H), 8.23 (s, 2H), 8.14 (d, *J* = 8.8 Hz, 2H), 7.94 (d, *J* = 8.8 Hz, 2H), 7.74 (d, *J* = 8.8 Hz, 2H), 7.61 (d, *J* = 8.8 Hz, 2H), 7.53 (d, *J* = 8.8 Hz, 2H), 6.84 (d, *J* = 8.8 Hz, 2H); *m/z* = 529.7838 $[M + K]^+$; IR (KBr): ν_{max} (in cm^{-1}) = 3356 (N-H stretching, asymmetric), 3205 (N-H stretching, symmetric), 1671(s), 1602(s), 1522(s), 1261 (C-N stretching) and 754 (NH_2 wagging). The ^{13}C NMR spectrum of derivative **4** could not be recorded due to its poor solubility.

Generation of PANI-5@Au:CuO NCS:

(a) PANI-5@Au:CuO (1:1) NCS

Solutions of 54 μL of Au^{3+} (0. 1 M) and 180 μL of Cu^{2+} (0.1 M) ions were simultaneously added to 12 mL of aggregates of derivative **4** (10^{-4} M) in H_2O-THF (6:4) solvent mixture with vigorous stirring. During stirring, the color of solution changed from light yellow to green and finally dark brown indicating the generation of PANI-**5**@Au:CuO NCS. Brown colored precipitates were observed after stirring the reaction mixture continuously for 1h at room temperature. The resulting reaction mixture was sonicated to obtain homogeneous solution.

(b) PANI-5@Au:CuO (1:2) NCS

Solutions of 54 μL of Au^{3+} (0. 1 M) and 360 μL of Cu^{2+} (0.1 M) ions were simultaneously added to 15 mL of aggregates of derivative **4** (10^{-4} M) in H_2O-THF (6:4) solvent mixture with vigorous stirring for 1h at room temperature. 4.0 mL of this solution was used as such for carrying out sequential amination/azidation/annulation reactions.

(c) PANI-5@Au:CuO (2:1) NCS

Solutions of 108 μL of Au^{3+} (0. 1 M) and 180 μL of Cu^{2+} (0.1 M) ions were simultaneously added to 15 mL of aggregates of derivative **4** (10^{-4} M) in H_2O-THF (6:4) solvent mixture with vigorous

stirring. 4.0 mL of this solution was used as such for carrying out sequential amination/azidation/annulation reactions.

General Procedure for Synthesis of Benzimidazole derivatives (8a-8k/8m/8n) using PANI-5 @Au:CuO nanocomposites.

In a 50 mL round-bottom flask (RBF), aniline **7a** (0.1 g, 1.0 mmol), $TMSN_3$ (2.0 mmol) and methyl benzene **6a** (10 mmol) were mixed in DMSO (10 mL) in the presence of PANI-**5**@Au:CuO NCS (0.01 mmol). The reaction mixture was degassed under vacuum for 2-3 min and then irradiated with a 100 W tungsten filament bulb (0.24 W/cm^2) from a distance of 10 cm to provide visible light for 12 h. The reaction temperature was maintained at room temperature by putting RBF in a water bath. After completion of the reaction, the reaction mixture was stirred with saturated Na_2SO_3 (1 mL) for 1 h and extracted with ethyl acetate. The organic layer was washed with brine, dried over anhydrous Na_2SO_4 and distilled off to yield a residue that was purified by column chromatography using hexane and ethyl acetate as an eluent to afford desired products. The aqueous layer containing nanocomposites was then used as such for further catalytic reactions.

Table S1. Comparison of wet chemical method in present manuscript over other reported procedure in the literature for the preparation of Au-CuO nanocomposites.

Journal	Nano composites	Preparation method	Chemicals used	External Reducing/ oxidising agent/ Surfactant/ Base	Temp (^{o}C)	Time	Application	Shape	Size	Re-cyclability of catalyst
Present Manuscript	**PANI-5@Au-CuO nanocomposites**	**Wet Chemical Method**	**Pentacenequinone derivative 4, Gold Chloride, $CuCl_2.2H_2O$**	**No**	**Room temperature**	**70 min.**	**Construction of 2-arylbenzimidazoles *via* sequential amination/ azidation/ annulation strategy**	**Irregular**	**20 nm**	**Three Times**
J. Am. Chem. Soc., **2017**, *139*, 8846	Au/CuO	Thermal decomposition method	$Cu(acac)_2$, tetralin, TBAB, Oleylaamine $HAuCl_4.3H_2O$	Yes	250°C	3h	CO oxidation reaction	Spherical	8.2-8.4 nm	**Two times**
Nanoscale, **2017**, *9*, 15033	Au-CuO nanoparticles	Co-reduction method	Dry Al_2O_3, $NaBH_4$, $HAuCl_4.3H_2O$, PVA, urea, $Cu(NO_3)_2.3H_2O$	Yes	300°C	3h	CO oxidation reaction	Spherical	5.4 nm	-
RSC Adv., **2016**, *6*, 81607	Au-CuO nanohybrids	Wet Chemical Method	$N_2H_4.H_2O$, $NaBH_4$, $Cu(NO_3)_2$, PVP, $(NH_3.H_2O)$, NaOH, $HAuCl_4.4H_2O$, L-ascorbic acid, Trisodium citrate	Yes	80°C	4.5 h	Degradation of Rhodamine B	Nanoflakes	100 nm	Five times
Sci. Rep. **2015**, *5*,16115	Au/CuO	Electrochemical method	Copper foil, $HAuCl_4$, 3 M NaOH	Yes	180°C	2 h	Glucose detection	Cauliflower	500 nm	-
RSC Adv., **2015**, *5*, 9130	Au/CuO	Thermal reduction method	$Cu(NO_3)_2.5H_2O$, glucose, NaOH, $K_3[Fe(CN)_6$, uric acid, Aminoethanol, $NaAuCl_4.4H_2O$, Ascorbic Acid, Sodium citrate	Yes	200^{o}C	2-4 h	Glucose sensor and CO oxidation	Nanosheets	140-200 nm	-

Table S2. Comparison of catalytic activity of PANI-5@Au:CuO NCS with other transition metal based catalytic systems reported in literature for synthesis of 2-substituted benzimidazoles.

Journal Name	Catalyst	Catalyst loading	Ligand/base/Oxidant/ Pressure of gas	Solvent	Temperature	Time	Yield
Present Manuscript	**PANI-5@Au:CuO NCS**	0.01 mmol	-	DMSO	Visible light	10-18 h	61-87%
***Chem. Commun.*, 2019**, *55*, 5958-5961	$NiCl_2$	2.5 mol%	1,10-Phenanthroline, *t*-BuOK	Toluene	140^0C	24 h	30-52%
J. Org. Chem. ***2018***, *83*, *9553*	tridentate NNS ligand based manganese (I) complex	0.05 mmol	t-BuOK	neat	140^0C under argon atmosphere	20 h	50-91%
ChemCatChem, 2018, **10**, 1607	Ru (II)-NNN pincer complex	0.25 mol%	$NaBPh_4$, dppe	neat	165^0C	24 h	18-96%
Sci. Rep., **2017**, *7*, 43758	CuI	10 mol%	Ph_3P, K_2CO_3	DMF	135^0C	24 h	75-85%
ACS Catal., **2017**, *7*, 7456	Co-PNNH complex	5 mol%	$NaHBEt_3$, *t*-BuOK, $4A^0$ MS	Toluene	150^0C	24 h	28-99%
Org. Lett., **2017**, *19*, 6554	$Cu(OAc)_2$	20 mol%	TBHP	DMSO	80^0C	12-25 h	43-77%
Org. Lett., **2017**, *19*, 4343	$[Cp^*IrCl_2]_2$	4 mol%	$AgNTf_2$, Phenylacetic acid	DCE	80^0C	12 h	30-99%
Org. Lett. **2017**, 19, 3243	$[Cp^*IrCl_2]_2$/ $AgNTf_2$	2.5/10 mol%	PiVOH	DCE	100^0C	24 h	40-87%
J. Org. Chem. **2017**, 82, 9243	$[Rh(COD)Cl]_2$	5 mol%	dAr^Fpe, K_3PO_4	Toluene	120^0C	24 h	5-97%
***Org. Chem. Front.*, 2017**, **4**, 392	$Pd(OAc)_2$	0.1 mmol	$FeCO_5$	Ethanol	Microwave irradiation, 100^0C	20 min	65-88%
Dalton Trans., 2017, **46**, 15012	RuHCl(CO)(PNS(O) complex	0.2 mol%	$NaBPh_4$	neat	165^0C	12 h	64-85%
Angew. Chem. Int. Ed., **2016**, 55, 15175	Co-SiCN nanocomposite	5.0 mol%	5.0 MPa hydrogen pressure	Triethylamine	110^0C	24 h	68-91%
Catal. Sci. Technol., **2016**, **6**, 1677	Ir/TiO_2-500	0.010 mmol	-	Mesitylene	120^0C under argon atmosphere	18 h	54-99%
J. Org. Chem., **2015**, *80* , 6102	$CuCl_2 \cdot H_2O$	0.2 equiv.	Bipy, K_2CO_3, O_2 (1atm)	Toluene	100^0C	24 h	27-81%

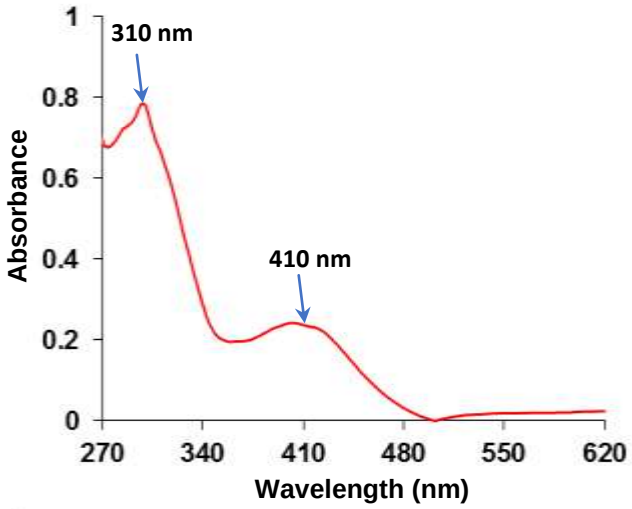

Figure S1 UV-vis spectrum of compound **4** in pure THF.

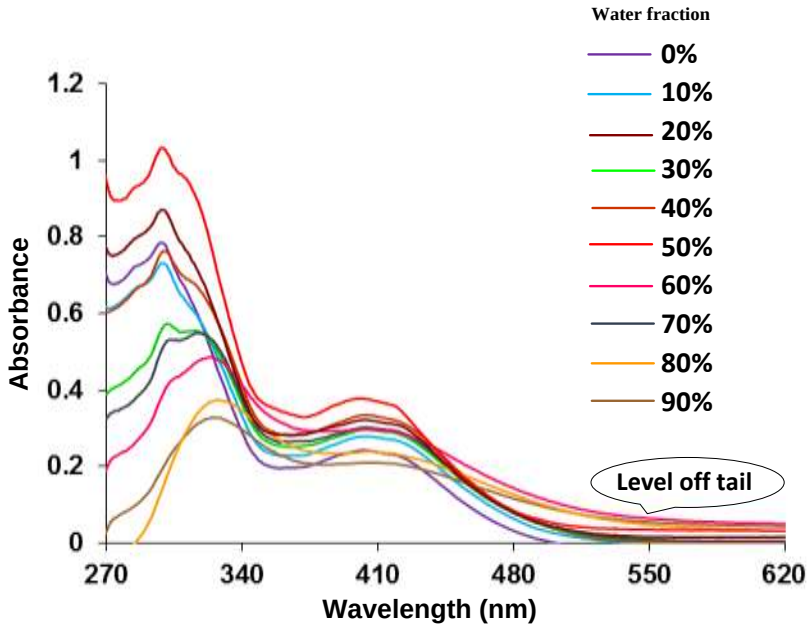

Figure S2 UV-vis spectra showing the variation in absorbance of compound **4** (10 μM) in H_2O-THF mixture with different fractions of H_2O.

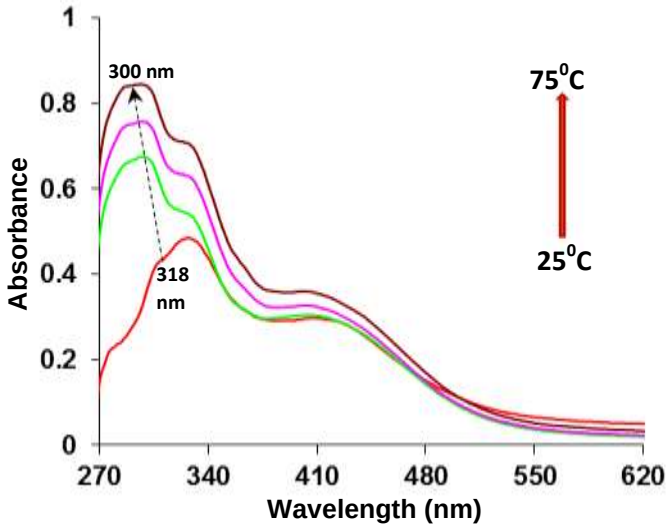

Figure S3 UV-vis absorption spectra of compound **4** in H_2O-THF (6:4) solvent mixture upon increasing temperature from 25 to 75°C.

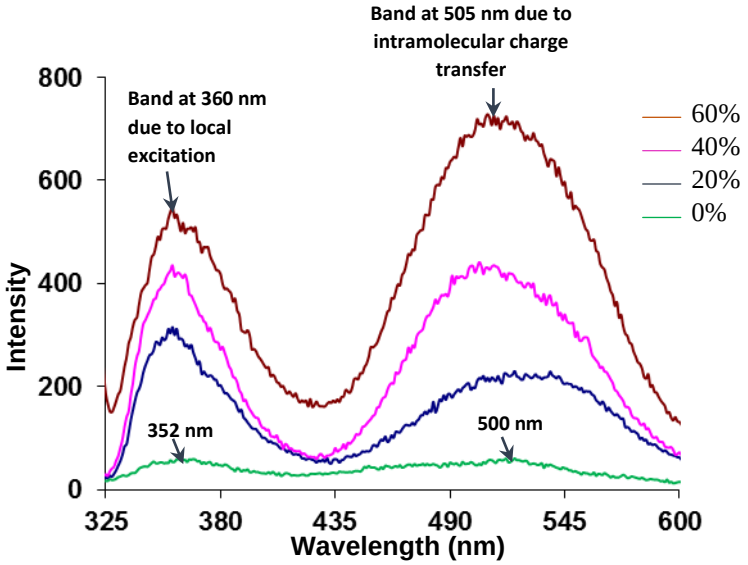

Figure S4 Fluorescence spectra of compound **4** (10 μM) in H_2O-THF mixture with different water fractions; λ_{ex} = 310 nm

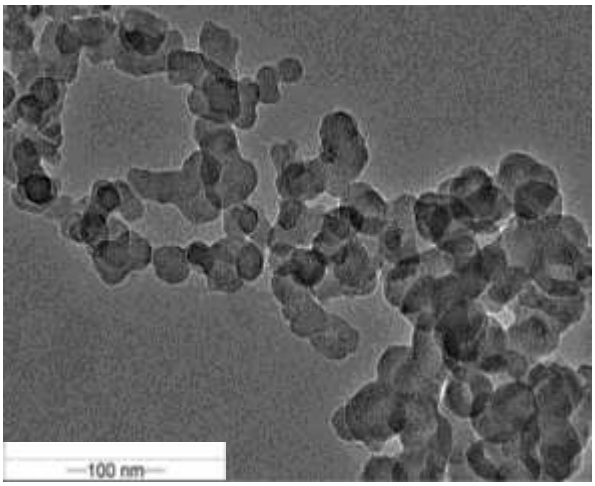

Figure S5 TEM image of compound **4** in H_2O-THF (6:4) solvent mixture showing formation of aggregates having irregular shape; scale bar 100 nm.

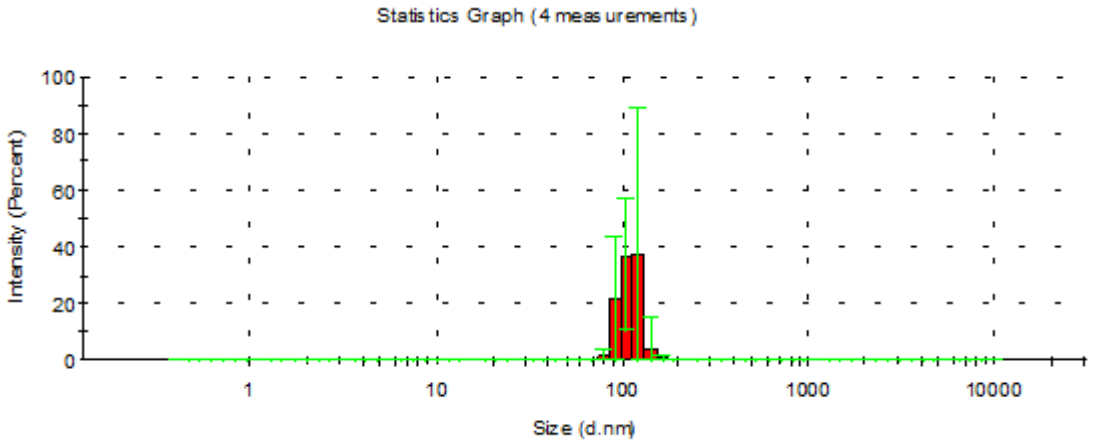

Figure S6 DLS studies of compound **4** in H_2O-THF (6:4) mixture which showed the presence of irregular shaped particles.

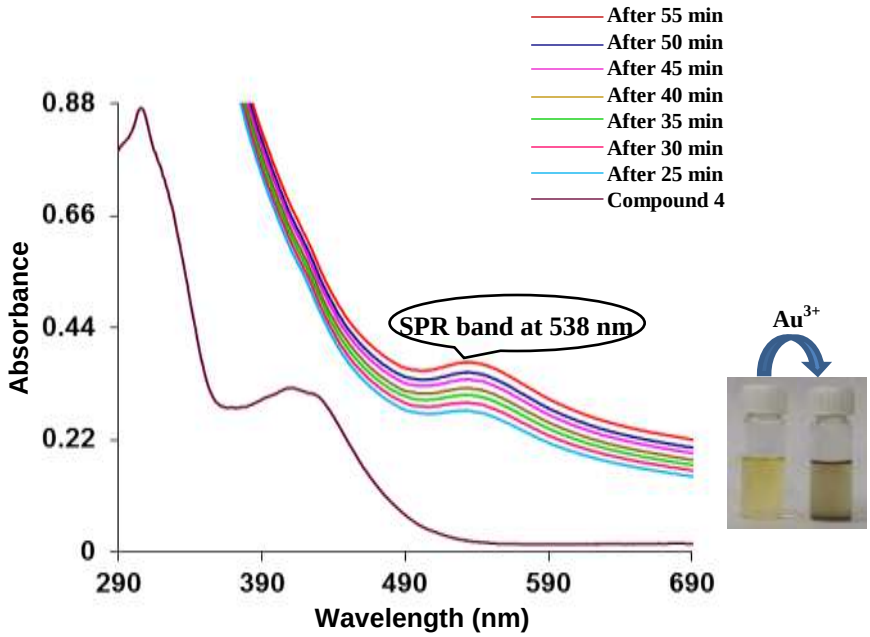

Figure S7 UV-vis spectra of compound **4** (10 μM) upon addition of Au^{3+} ions (18 equiv.) with time in H_2O-THF (6:4) solvent mixture showing surface plasmon resonance (SPR) band at 538 nm. Inset showing change in color of solution of aggregates of compound **4** from yellow to blackish-brown with addition of Au^{3+} ions.

Regression Statistics	
Multiple R	0.998222
R Square	0.996448
Intercept	0.196286
Slope	0.003136

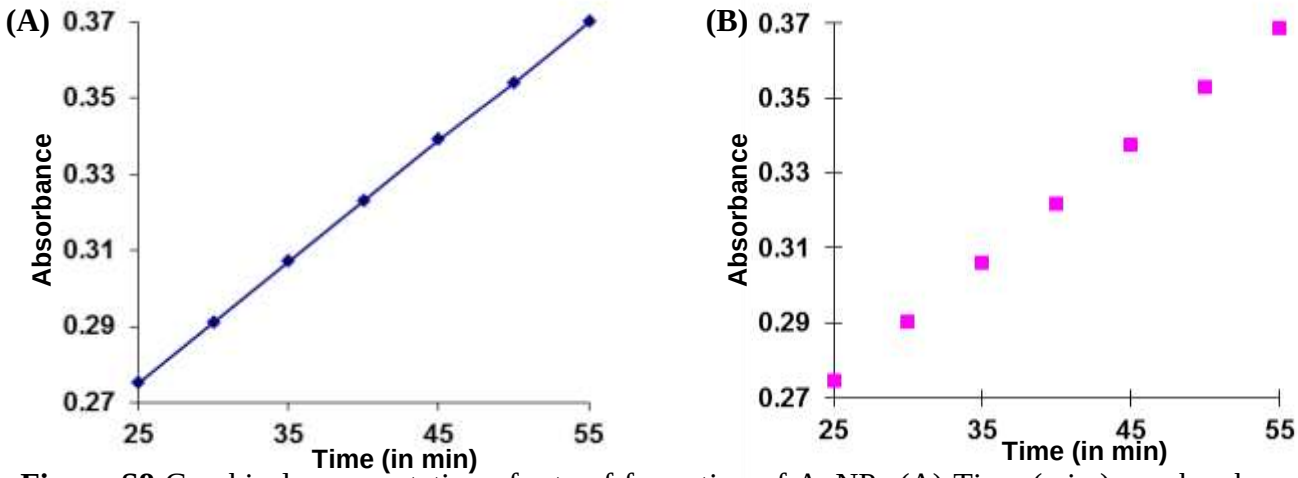

Figure S8 Graphical representation of rate of formation of AuNPs (A) Time (min.) *vs*. absorbance plot at 538 nm (B) regression plot of A.

The first order[2] rate constant for the formation of gold nanoparticles was calculated from the change in intensity of absorbance of assemblies of derivative **4** at 538 nm wavelength in the presence of Au^{3+} ions at different time interval.[3] From the time *vs*. absorbance plot at fixed wavelength 570 nm by using first order rate equation, we get the rate constant = k = slope × 2.303 =1.20×10^{-4} sec.

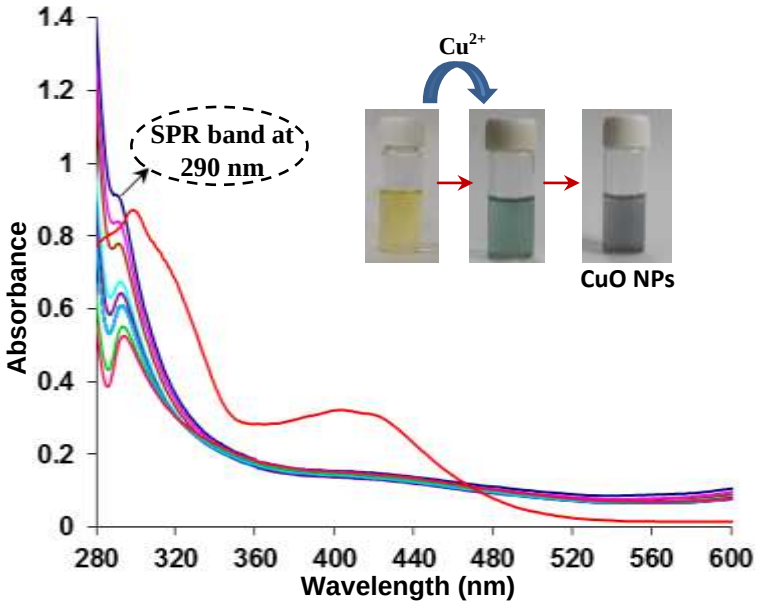

Figure S9 UV-vis spectra of compound **4** (10 μM) upon addition of Cu^{2+} ions (60 equiv.) with time in H_2O-THF (6:4) solvent mixture showing surface plasmon resonance (SPR) band at 290 nm. Inset showing change in color of solution of aggregates of compound **4** from yellow to blue and finally to black with addition of Cu^{2+} ions

Regression Statistics	
Multiple R	0.997032
R Square	0.994073
Intercept	0.1551
Slope	0.01043

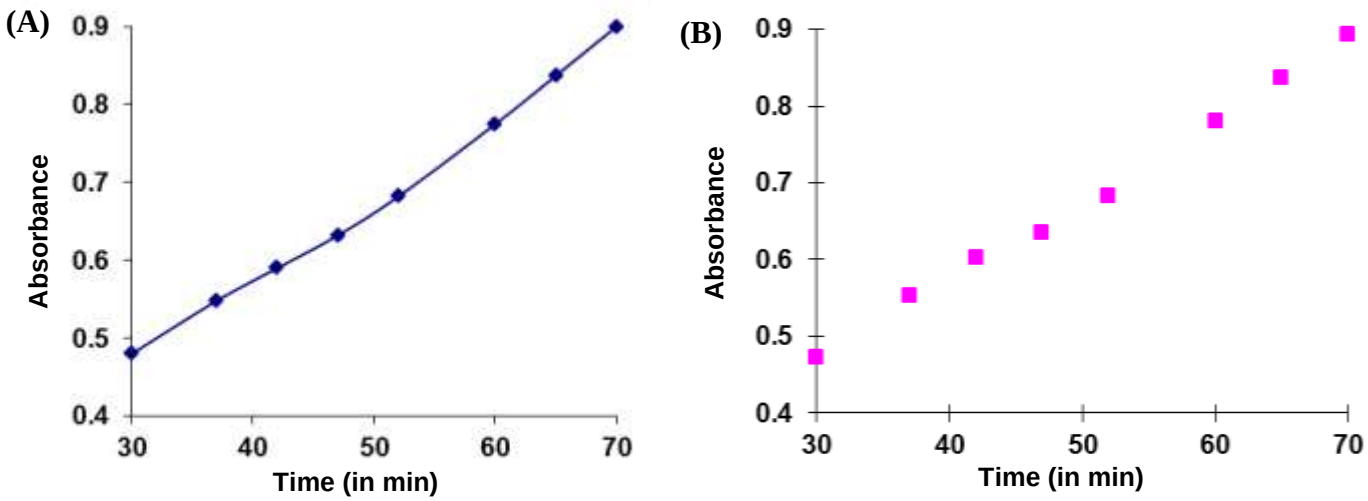

Figure S10 Graphical representation of rate of formation of CuO NPs (A) Time (min.) *vs*. absorbance plot at 290 nm (B) regression plot of A.

The first order[2] rate constant for the formation of CuO NPs was calculated from the change in intensity of absorbance of assemblies of compound **4** at 290 nm wavelength in the presence of Cu^{2+} ions at different time interval .[3] From the time *vs*. absorbance plot at fixed wavelength 290 nm by using first order rate equation, we get the rate constant = k = slope × 2.303 = 4.0×10^{-4} sec^{-1}.

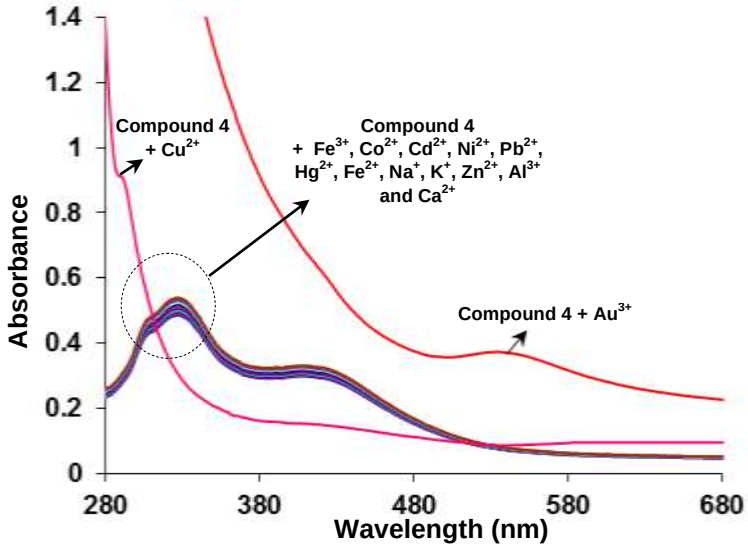

Figure S11 Absorption spectra of compound **4** (10 μM) upon addition of 60 equivalents of various metal ions (Au^{3+}, Cu^{2+}, Fe^{3+}, Co^{2+}, Cd^{2+}, Ni^{2+}, Pb^{2+}, Hg^{2+}, Fe^{2+}, Na^{+}, K^{+}, Zn^{2+}, Al^{3+} and Ca^{2+}) as their chloride salts in H_2O-THF (6:4), buffered with HEPES, pH = 7.0.

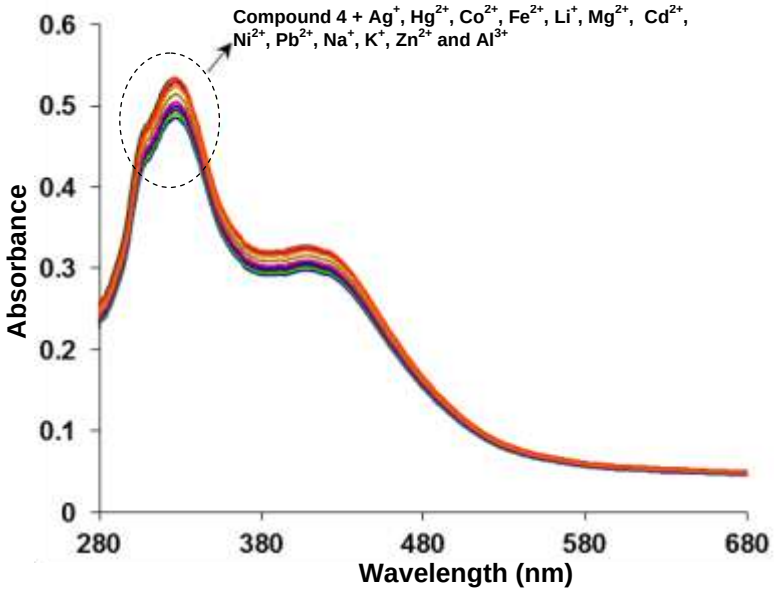

Figure S12 Absorption spectra of compound **4** (10 μM) upon additions of 60 equivalents of various metal ions (Ag^{+}, Hg^{2+}, Co^{2+}, Fe^{2+}, Li^{+}, Mg^{2+}, Cd^{2+}, Ni^{2+}, Pb^{2+}, Na^{+}, K^{+}, Zn^{2+} and Al^{3+}) as their perchlorate/nitrate salts in H_2O-THF (6:4), buffered with HEPES, pH = 7.0.

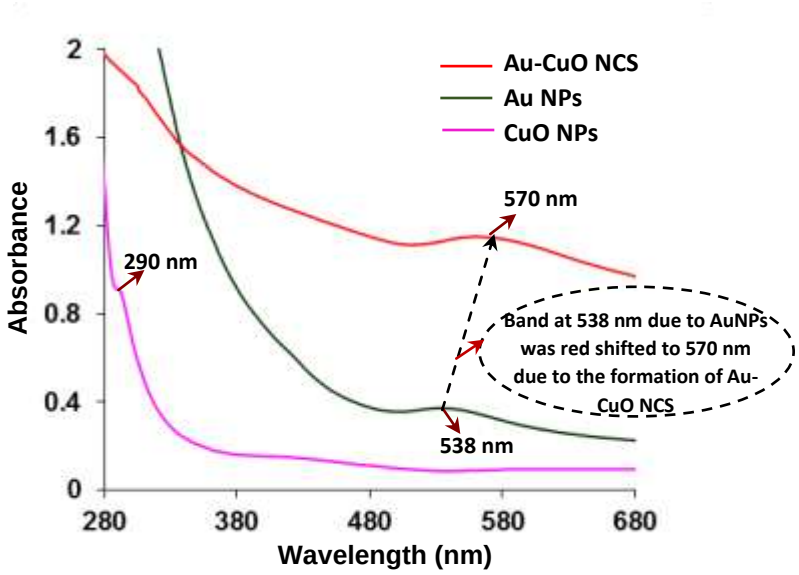

Figure S13 UV-vis spectra of aqueous solution of Au-CuO NCS (red line), Au NPs (green line), CuO NPs (pink line) stabilized by assemblies of compound **4**.

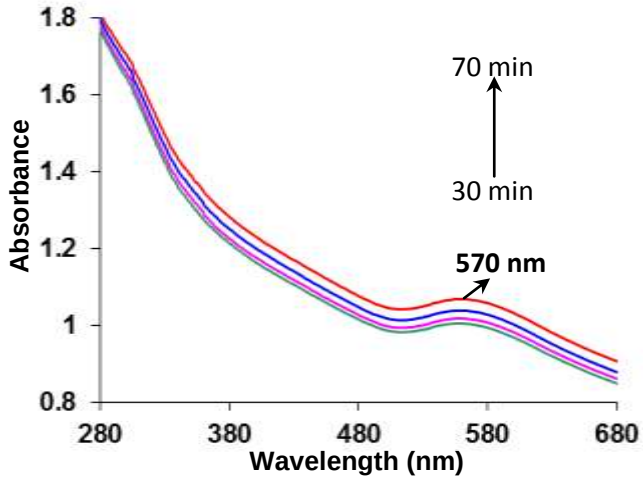

Figure S14 UV-vis spectra with time for simultaneous addition of aqueous solution of Au^{3+} and Cu^{2+} ions to the assemblies of compound **4**.

Regression Statistics	
Multiple R	0.999814
R Square	0.999628
Intercept	0.958057
Slope	0.001451

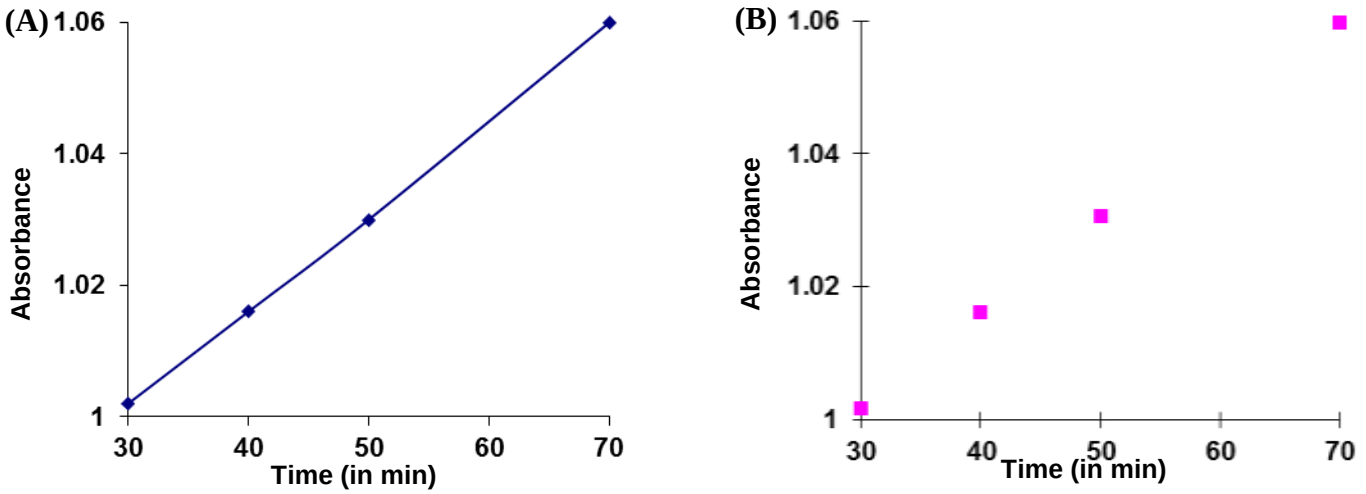

Figure S15 Graphical representation of rate of formation of Au-CuO NCS (A) Time (min.) *vs.* absorbance plot at 570 nm (B) regression plot of A.

The first order[2] rate constant for the formation of Au-CuO nanocomposites was calculated from the changes in intensity of absorbance of assemblies of compound **4** at 570 nm wavelength in the presence of Au^{3+} and Cu^{2+} ions at different time interval.[3] From the time *vs.* absorbance plot at fixed wavelength 570 nm by using first order rate equation, we get the rate constant = k = slope × 2.303 = 5.57 ×10^{-5} sec^{-1}.

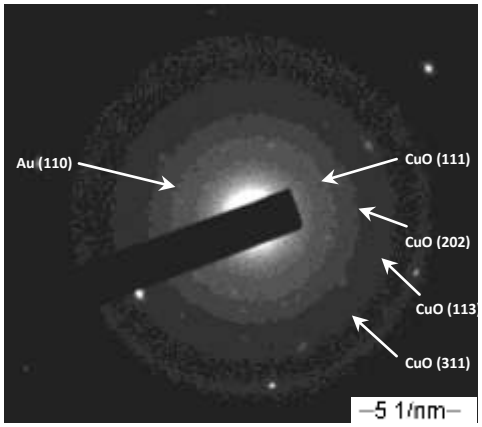

Figure S16 SAED pattern of PANI-**5**@Au:CuO NCS

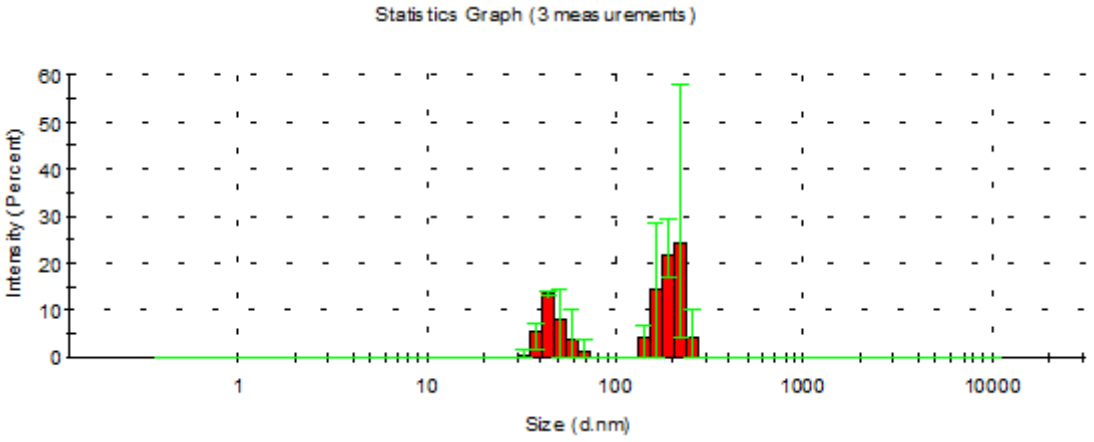

Figure S17 DLS studies of polymer supported bimetallic Au-CuO NCS indicated the presence of two sets of particles having size of about 43 nm and 220 nm.

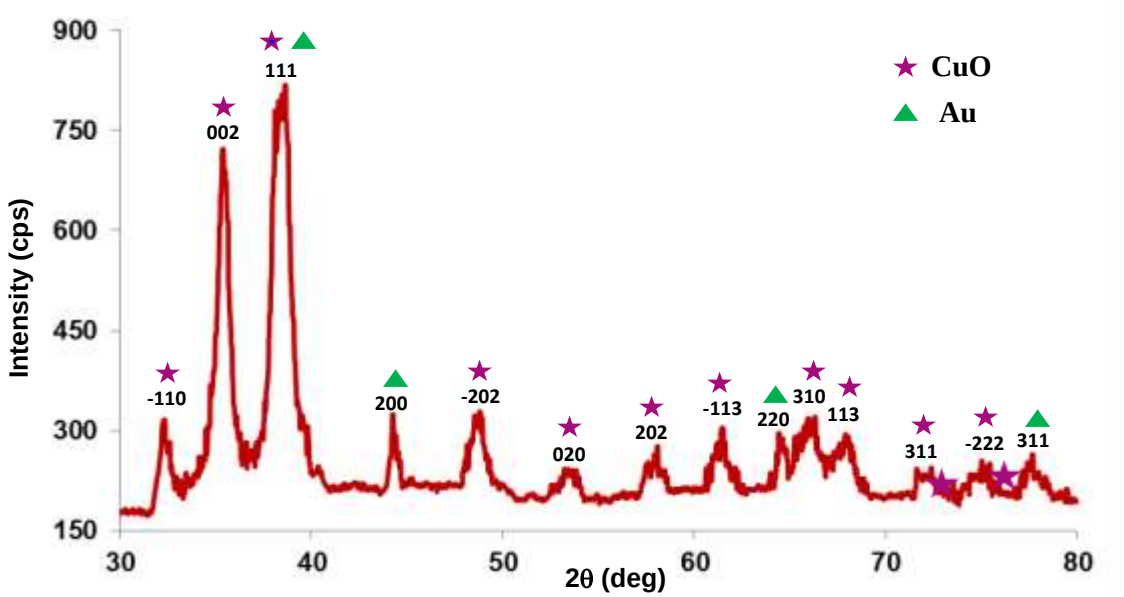

Figure S18 X-Ray diffraction pattern of *in situ* generated Au-CuO NCS.

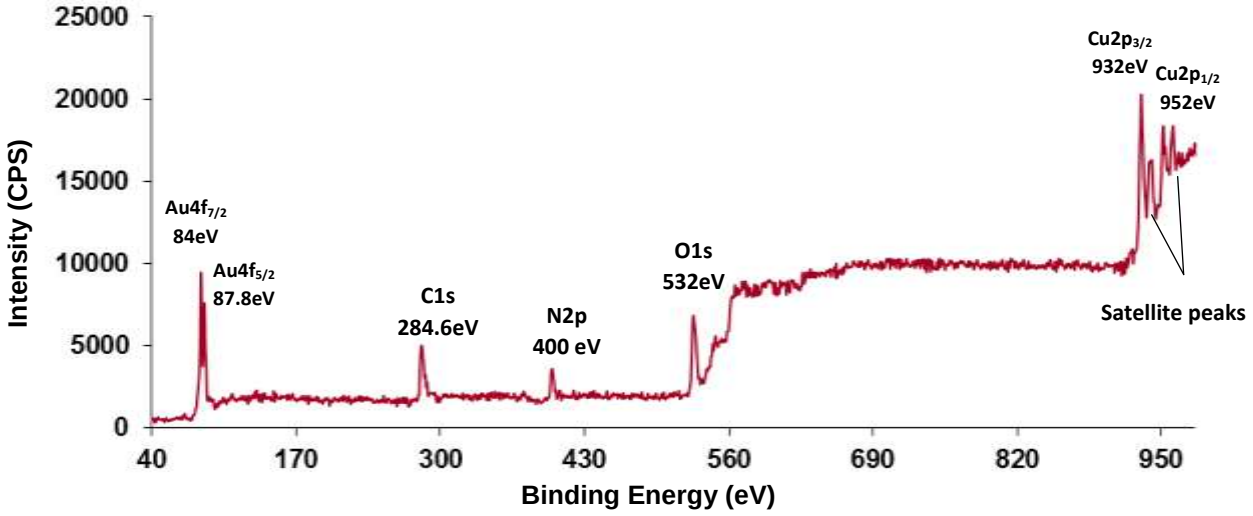

Figure S19 XPS analysis of PANI-**5**@Au:CuO NCS indicated the presence of Au^0 and CuO species along with polyaniline.

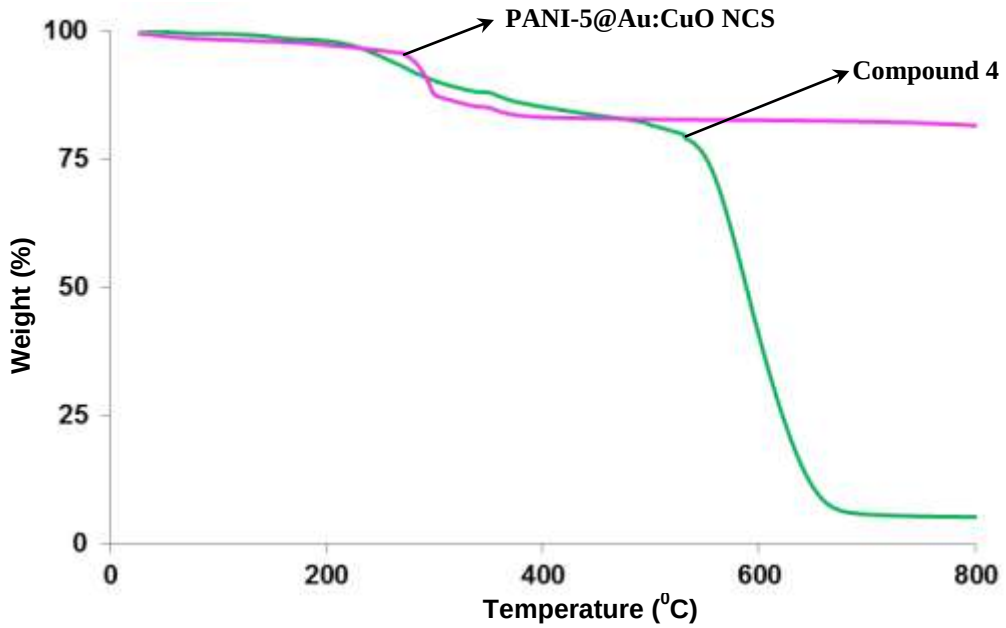

Figure S20 TGA of compound **4** and PANI-**5**@Au:CuO NCS

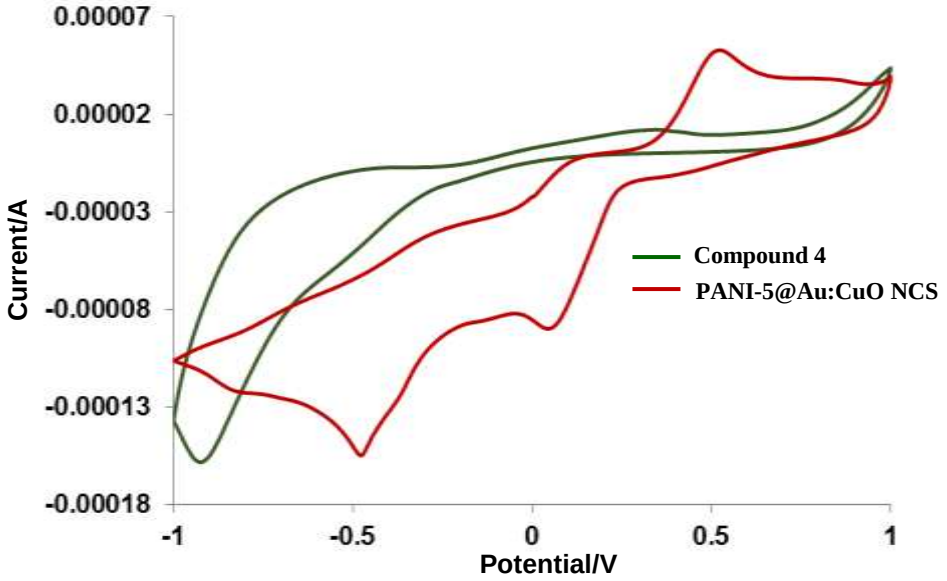

Figure S21 Cyclic voltammogram of the compound **4** and PANI-**5**@Au:CuO NCS in H_2O:CH_3CN (6:4) containing 0.1 M Bu_4NClO_4 (supporting electrolyte) and Ag/AgCl (reference electrode).

Table S3. Table showing oxidation and reduction potentials of compound **4** and **PANI-5@Au:CuO NCS**

Entry	Reduction potential (eV)	Oxidation potential (eV)
Compound 4	-0.91	0.35
PANI-5@Au:CuO NCS	-0.46	0.513

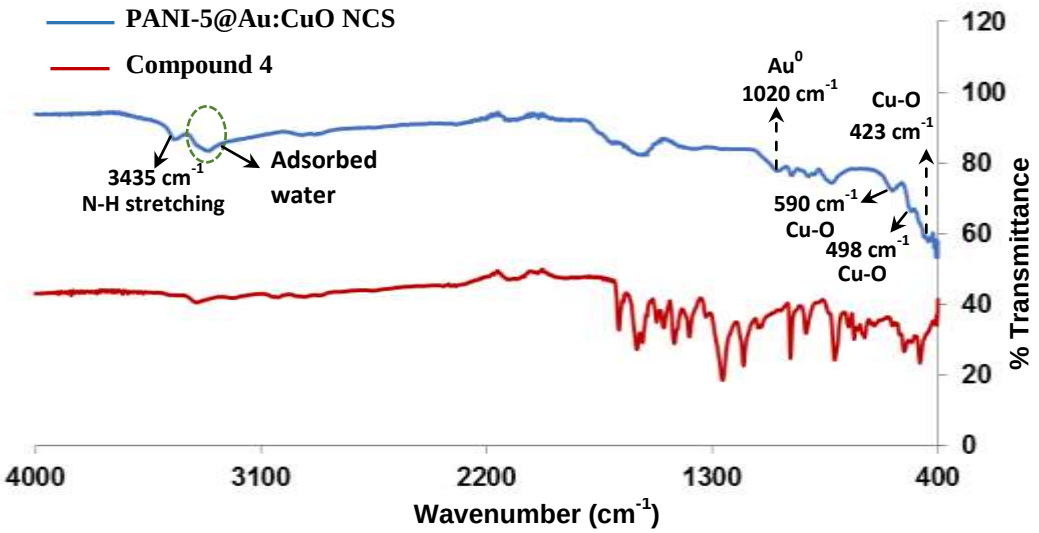

Figure S22 FT-IR spectra of compound **4** and PANI-**5**@Au:CuO NCS

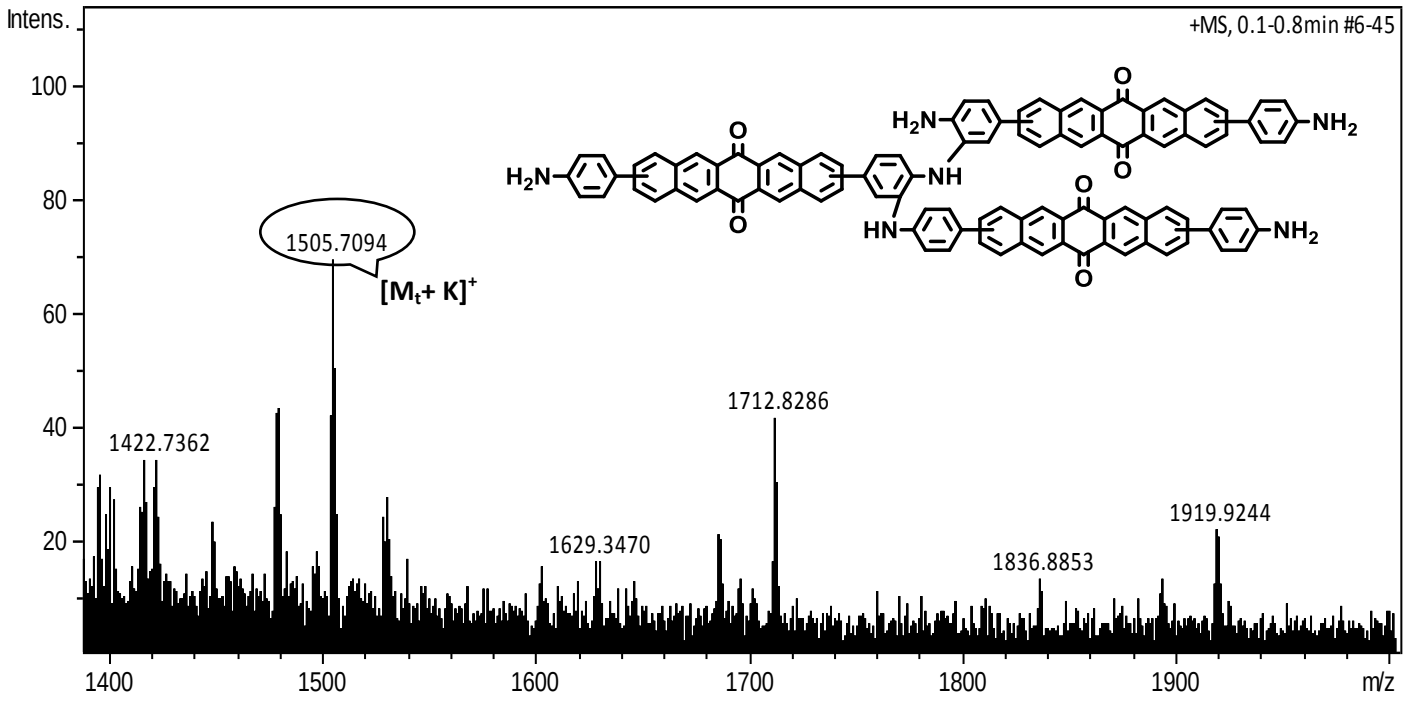

Figure S23 ESI-MS spectrum of trimer formed after oxidation of compound **4** showed a parent ion peak correspond to $[M_t + K]^+$, m/z = 1505.7094.

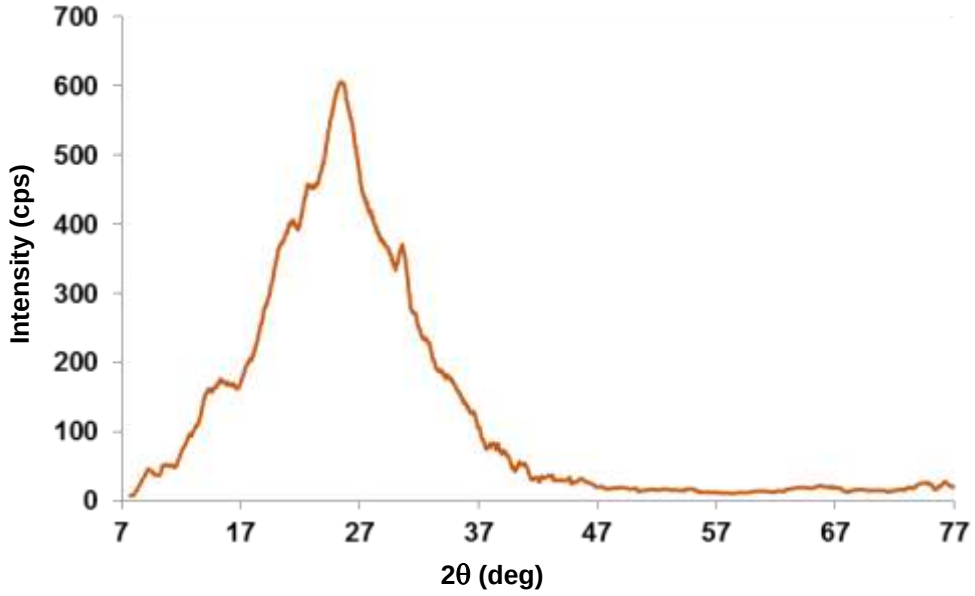

Figure S24 X-Ray diffraction pattern of polyaniline nanofibres **5**.

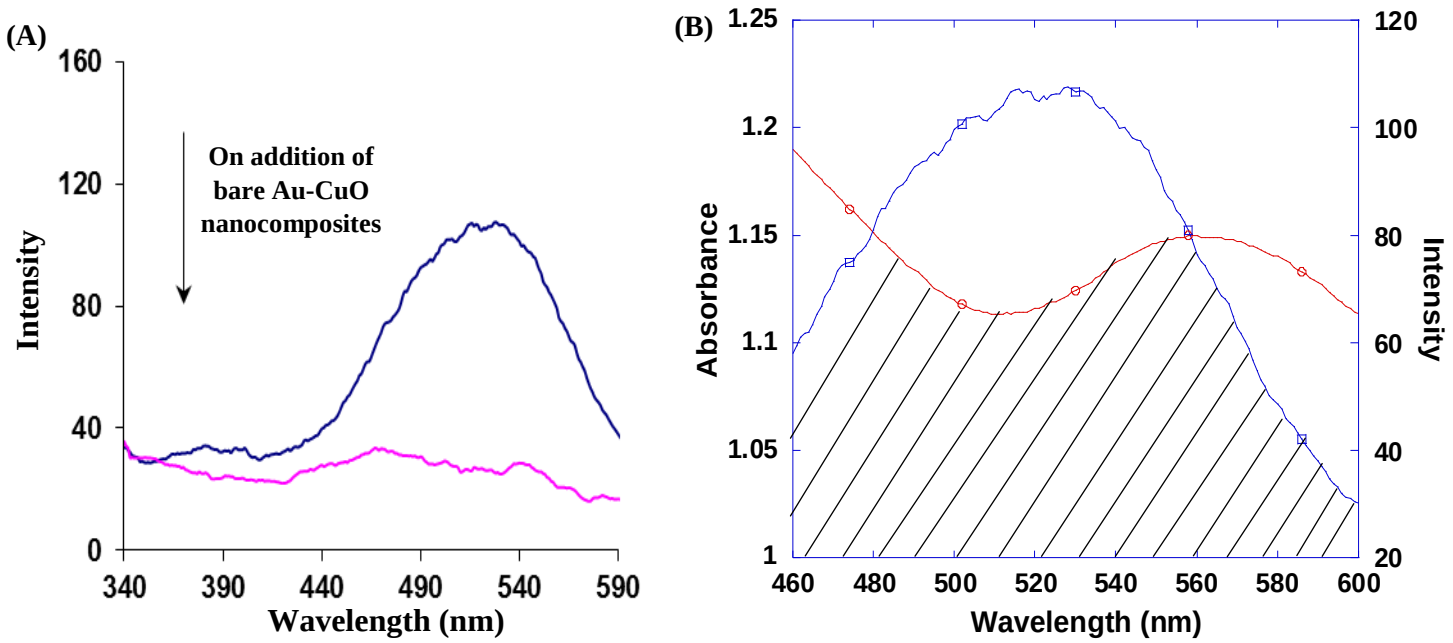

Figure S25 (A) Fluorescence spectra of oxidized species **5** in H_2O-THF (6:4) solvent mixture upon addition of bare Au-CuO nanocomposites (5 mol%); **(B)** Spectral overlap of absorption spectrum of Au-CuO NCS and fluorescence spectrum of oxidized species **5** in H_2O-THF (6:4) mixture showing energy transfer from oxidized species **5** to Au-CuO NCS.

Table S4. Selectivity for sequential amination, azidation and annulation reaction between toluene (6a) and aniline (7a) in the presence of $TMSN_3$ utilizing PANI-5@Au:CuO nanocomposites (1:1) as photocatalyst

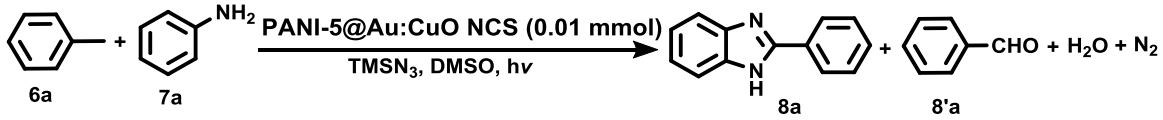

Entry	Amount (in mmol)		Selectivity[a] (%)	
	Benzimidazole (**8a**)	Benzaldehyde (**8'a**)	Benzimidazole (**8a**)	Benzaldehyde (**8'a**)
1.	0.768	0.130	85.5%	14.5%

[a]Selectivity (%)[4] : Amount of benzimidazole formed (mmol)/∑Amount of each product (mmol) X 100

Table S5. Screening data for sequential amination/azidation/annulation reaction between toluene (6a) and aniline (7a) in the presence of $TMSN_3$ utilizing various commercially available photocatalysts

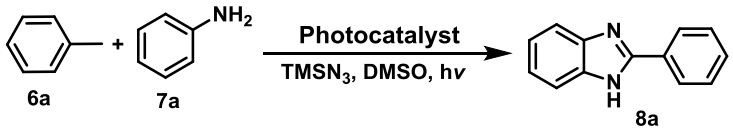

S. No.	Photocatalyst	Catalyst loading	Yield	Time
1.	**PANI@Au:CuO NCS (This Work)**	**0.01 mmol**	**72%**	**12 h**
2.	Rhodamine 6G	5 mol%	-	24 h
3.	Rhodamine B	5 mol%	-	24 h
4.	9-Fluorenone	5 mol%	-	24 h
5.	Methylene blue	5 mol%	-	24 h
6.	Fluorescein	5 mol%	-	24 h
7.	Alizarin	5 mol%	-	24 h

Table S6 Photocatalytic efficiency of PANI-5@Au:CuO prepared by mixing aggregates of derivative 4, Au^{3+} and Cu^{2+} ions in ratio of 2:1:1 for carrying out sequential amination, azidation and annulation reactions between toluene (6a) and aniline (7a) in presence of $TMSN_3$.

S. No.	PANI-5@Au:CuO NCS	Catalytic Cycle	Time (in h)	Yield of 8a
1.	Prepared by mixing aggregates of derivative **4**, Au^{3+} and Cu^{2+} ions in ratio of 2:1:1	Ist	14 h	70%
2.	Prepared by mixing aggregates of derivative **4**, Au^{3+} and Cu^{2+} ions in ratio of 2:1:1	5th	14 h	65%
3.	Prepared by mixing aggregates of derivative **4**, Au^{3+} and Cu^{2+} ions in ratio of 2:1:1	6th	14 h	63%
4.	Prepared by mixing aggregates of derivative **4**, Au^{3+} and Cu^{2+} ions in ratio of 2:1:1	7th	14 h	58%

Table S7. Effect of addition of TEMPO on sequential amination/azidation/annulation reaction utilizing PANI-5@Au:CuO NCS as photocatalyst

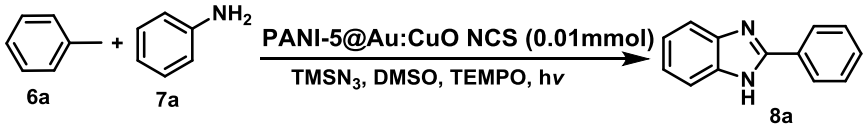

S. No.	TEMPO	Yield of 8a
1.	0.0 equiv.	72%
2.	1.0 equiv.	40%
3.	2.0 equiv.	12%

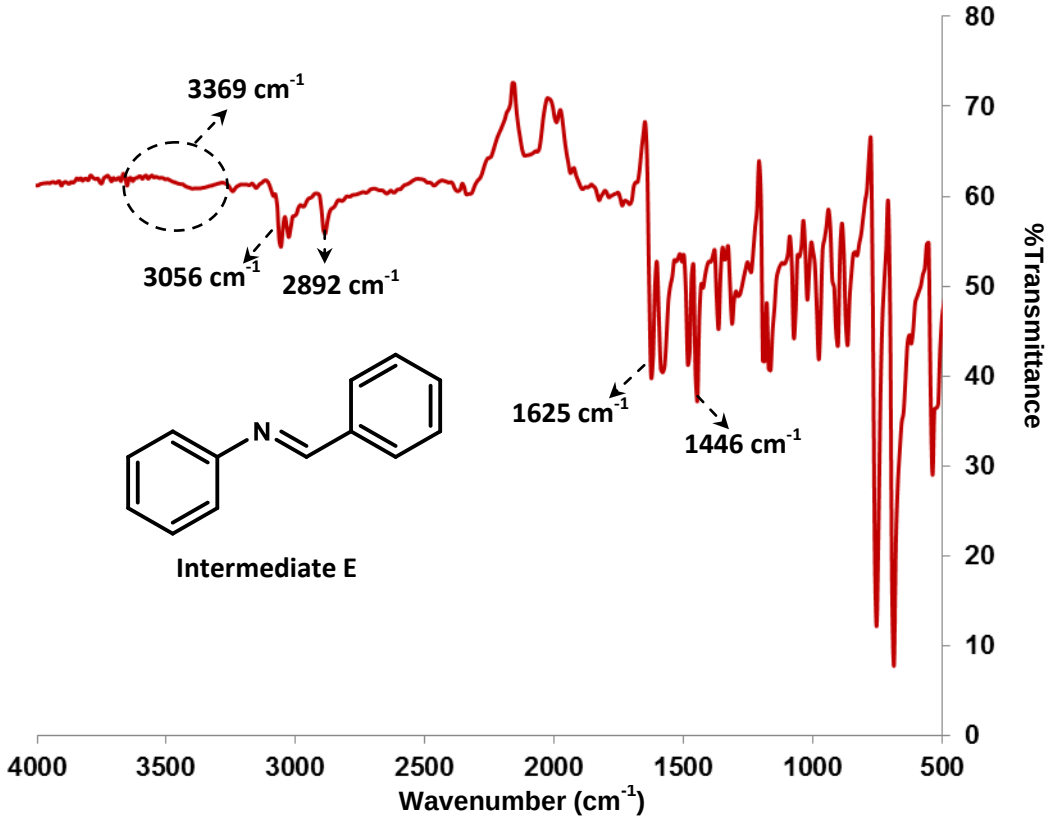

Figure S26 IR spectra of intermediate **E**.

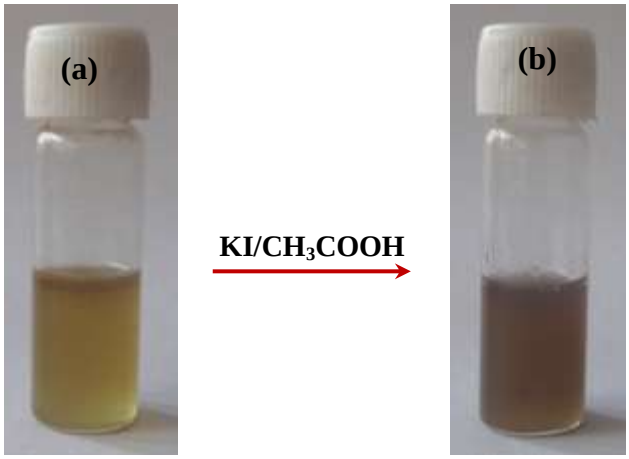

Figure S27 (a) Reaction mixture of aniline (1.0 mmol), toluene (10 mmol), $TMSN_3$ (2.0 mmol) and PANI-**5**@Au:CuO NCS (0.01mmol) as catalyst after irradiation of 8 h; (b) After addition of mixture containing KI (1.0×10^{-1}M) and aqueous acetic acid (1.0×10^{-1} M), color of solution changes to brown.

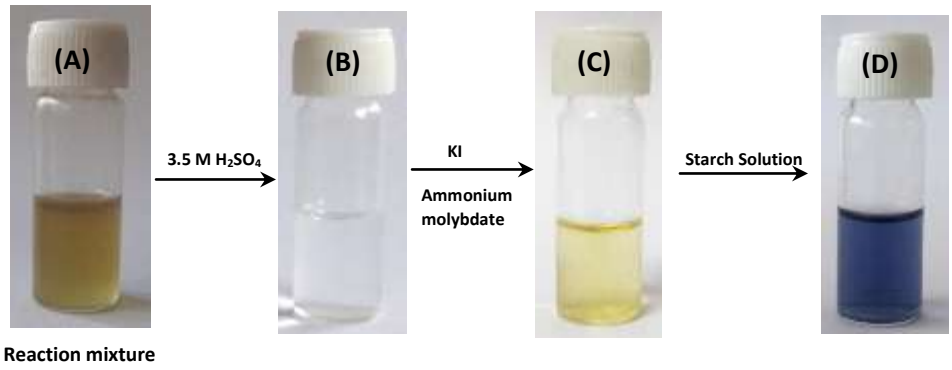

Figure S28 Iodometric test for detection of H_2O_2. (A) Reaction mixture; (B) Decolorization of reaction mixture on treatment with 3.5 M H_2SO_4; (C) Addition of 1% KI and 2 drops of ammonium molybdate changed the color of solution to yellow; (D) Addition of freshly prepared starch solution changed the color of solution to blue.

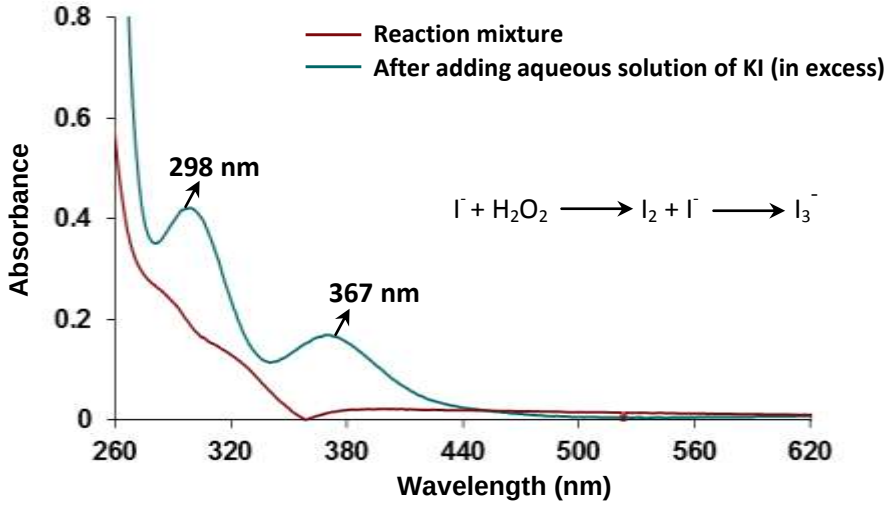

Figure S29 Detection of formation of H_2O_2 by monitoring the absorption spectra of I_3^- in aqueous media.

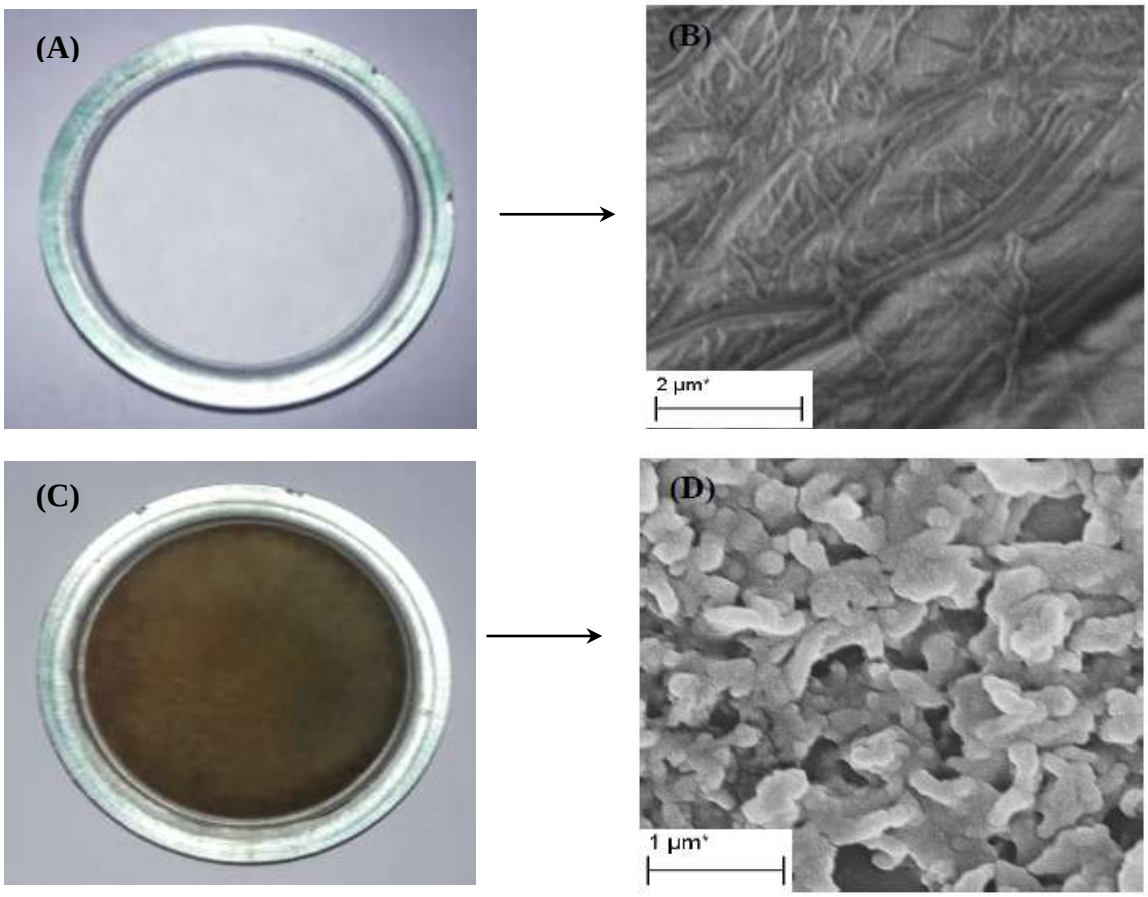

Figure S30 (A) Picture of the uncoated paper strip; (B) SEM image of uncoated paper strip; (C) Picture of dip coated paper strip with PANI-**5**@Au:CuO NCS; (D) SEM image of coated paper strip with PANI-**5**@Au:CuO NCS.

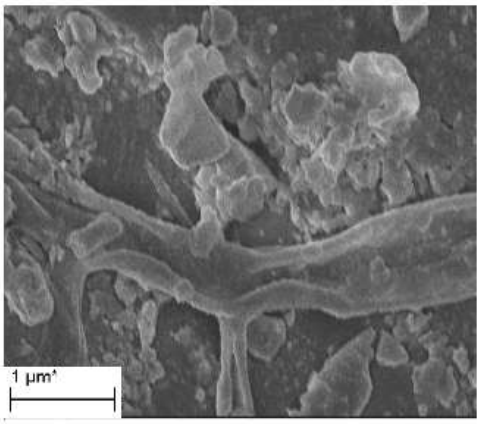

Figure S31 SEM image of recycled dip coated paper strip after three cycles.

Compound 8'a[5] Colorless liquid; Benzaldehyde: (0.014 g in 12% yield) .^{1}H NMR (400 MHz, $CDCl_3$, ppm) δ=10.03 (s, 1H), 7.90 (d, *J* = 7.2 Hz, 2H), 7.65 (t, *J* = 7.4 Hz, 1H), 7.55 (t, *J* = 7.4 Hz, 2H).

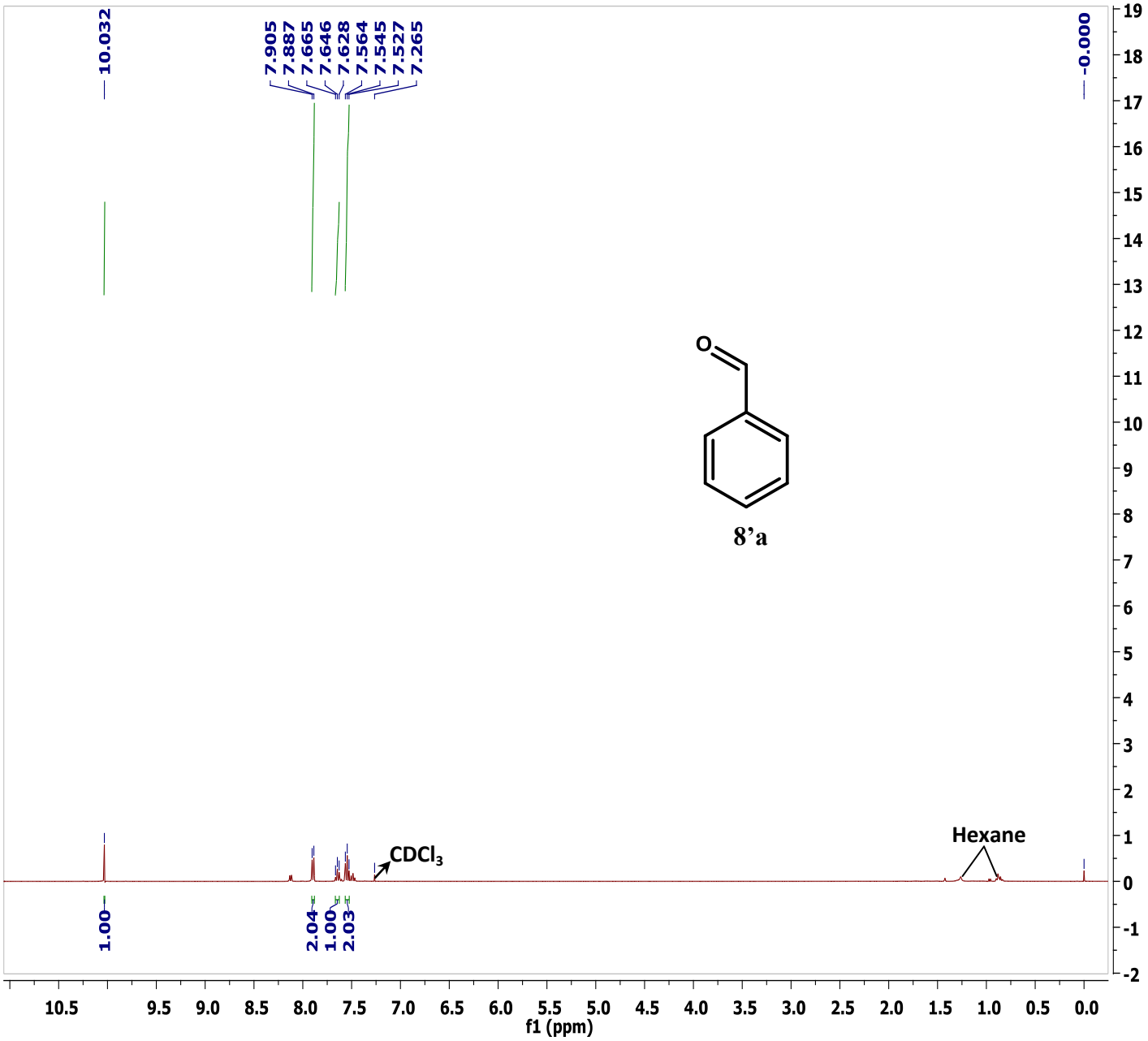

Figure S32 ^{1}H NMR spectrum of compound **8'a**

6a-Tempo adduct[6] Colorless oil; 1-(Benzyloxy)-2,2,6,6-tetramethylpiperidine: (0.106 g in 40% yield). ^{1}H NMR (300 MHz, $CDCl_3$, ppm) δ 7.36-7.27 (m, 5H), 4.84 (s, 2H), 1.60-1.48 (m, 6H), 1.26 (s, 6H), 1.16 (s, 6H)

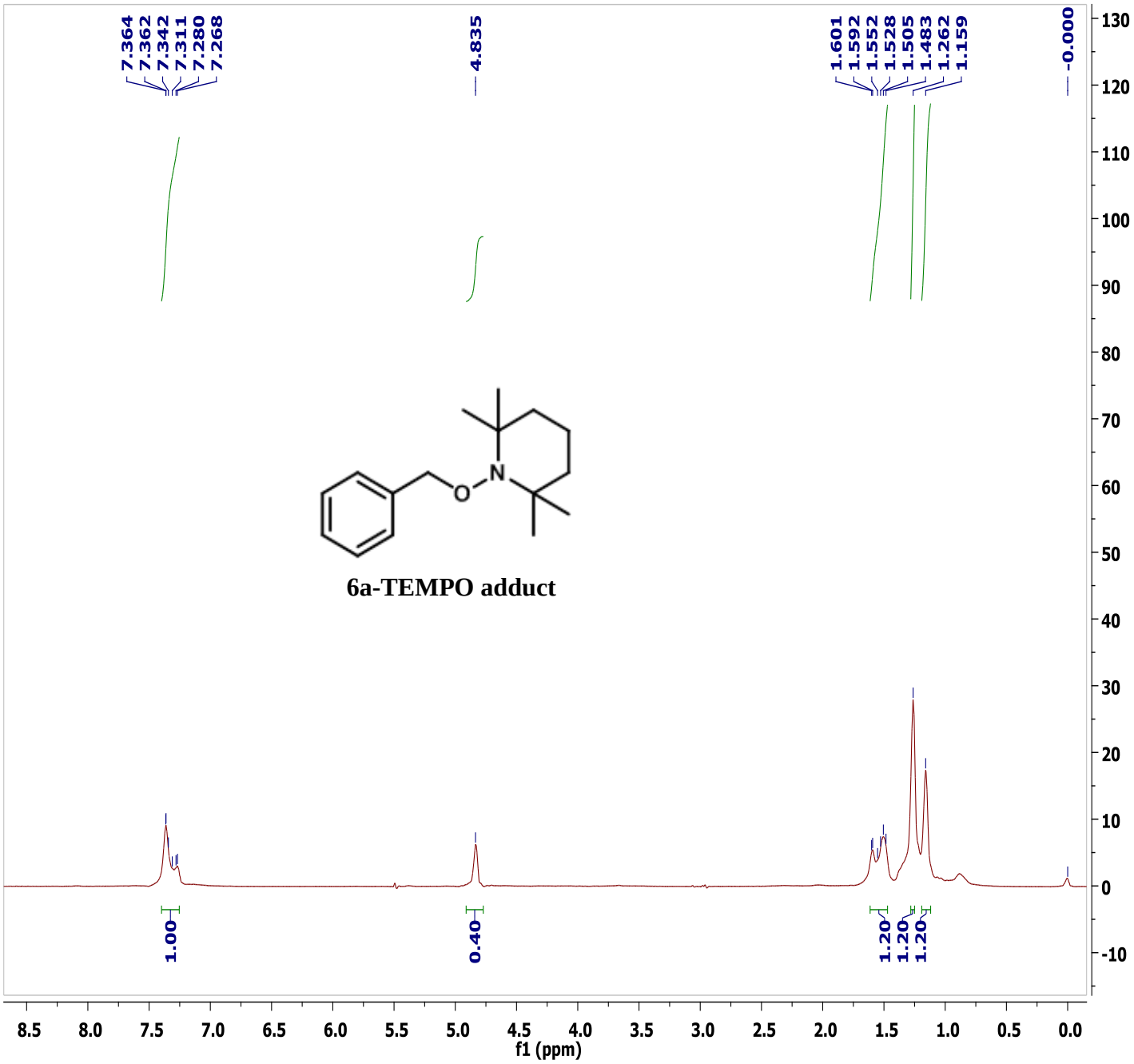

Figure S33 ^{1}H NMR spectrum of **6a-TEMPO** adduct

Compound 8a[7] White solid; 2-Phenylbenzimidazole: (0.149 g in 72% yield). ^{1}H NMR (500 MHz, DMSO-d_6, ppm): 12.90 (br s, 1H), 8.17 (d, *J* = 8.0 Hz, 2H), 7.66-7.48 (m, 5H), 7.21-7.20 (m, 2H).

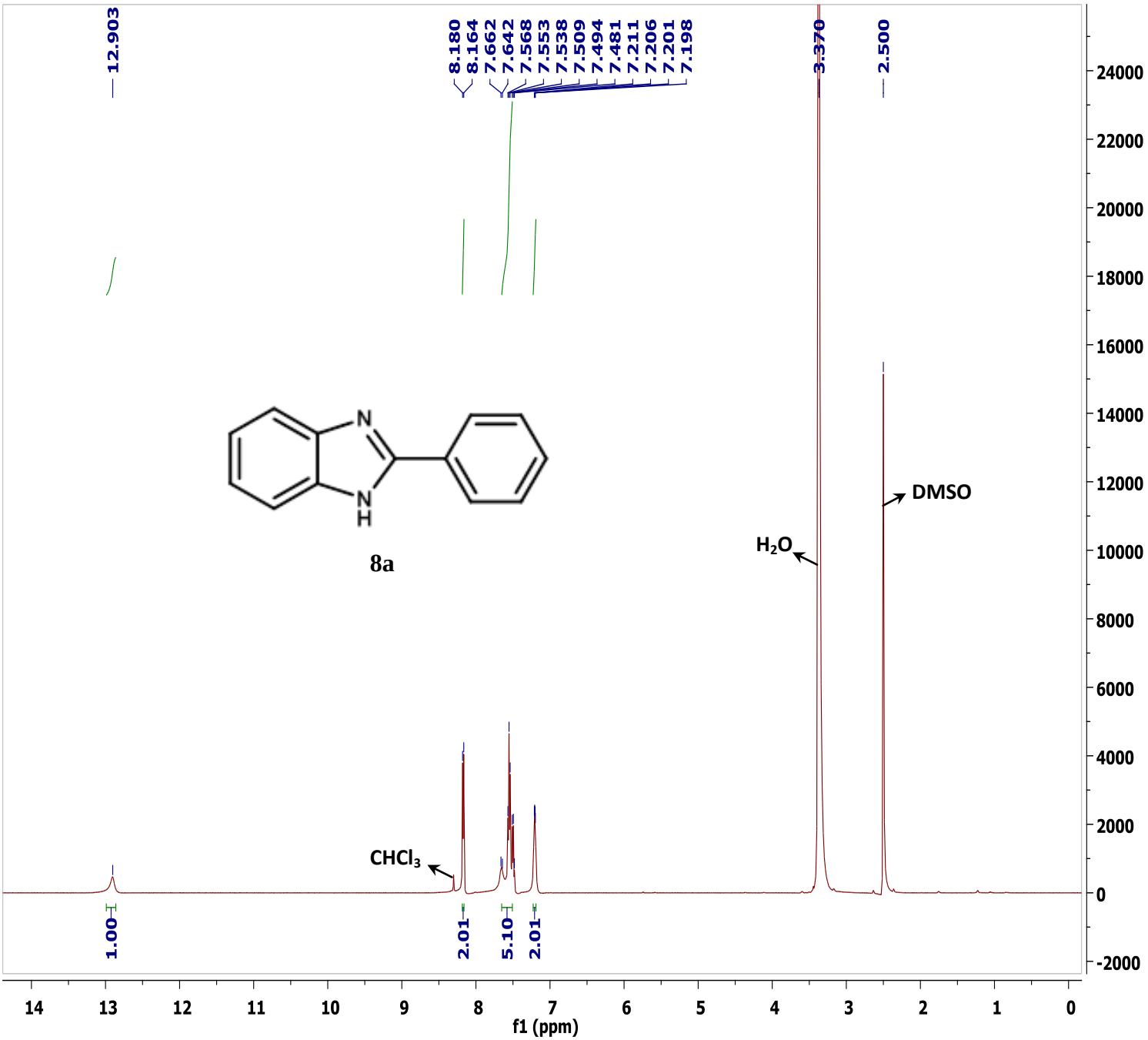

Figure S34 ^{1}H NMR spectrum of compound **8a**

Compound 8b[8] White solid; 2-(p-Tolyl)-1*H*-benzo[d]imidazole: (0.179 g in 80% yield). ^{1}H NMR (500 MHz, DMSO-d_6, ppm) δ 12.79 (br s, 1H), 8.06 (d, *J* = 8.5 Hz, 2H), 7.63 (d, *J* = 8.0 Hz, 1H), 7.50 (d, *J* = 8.0 Hz, 1H), 7.36 (d, *J* = 8.0 Hz, 2H), 7.21-7.16 (m, 2H), 2.38 (s, 3H)

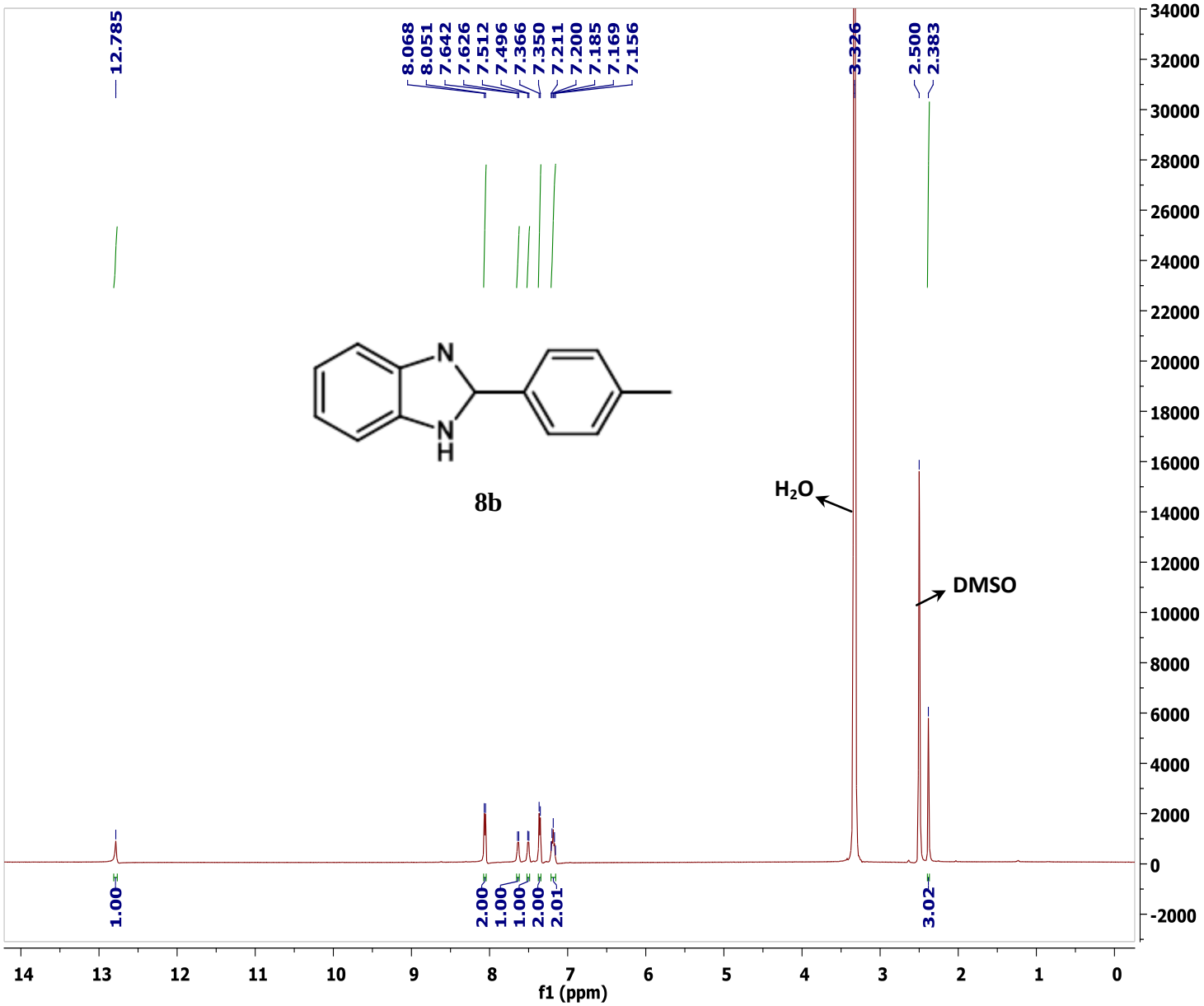

Figure S35 ^{1}H NMR spectrum of compound **8b**

Compound 8c[8] White solid; 2-(4-Methoxyphenyl)-1*H*-benzo[d]imidazole: (0.197 g in 82% yield). ^{1}H NMR (500 MHz, DMSO-d_6, ppm) δ 12.72 (br s, 1H), 8.11 (d, *J* = 8.5 Hz, 2H), 7.61 (d, *J* = 7.0 Hz, 1H), 7.49 (d, *J* = 7.0 Hz, 1H), 7.18-7.15 (m, 2H), 7.11 (d, *J* = 8.5 Hz, 2H), 3.84 (s, 3H)

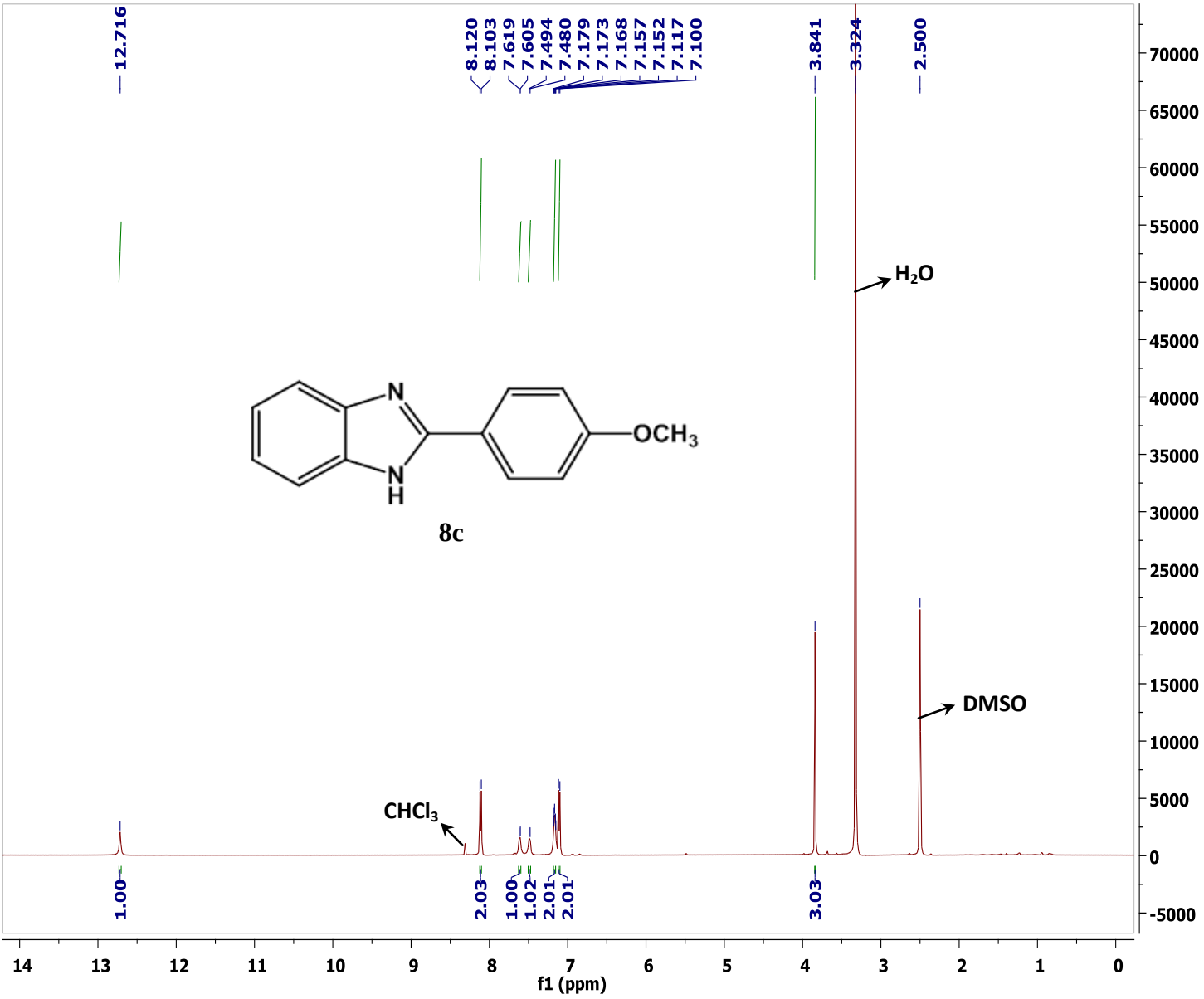

Figure S36 ^{1}H NMR spectrum of compound **8c**

Compound 8d[9,10] White solid; 2-(4-bromophenyl)-1*H*-benzo[d]imidazole: (0.188 g in 64% yield). ^{1}H NMR (500 MHz, DMSO-d_6, ppm) δ 12.99 (br s, 1H), 8.11 (d, *J* = 8.5 Hz, 2H), 7.77 (d, *J* = 8.5 Hz, 2H), 7.60 (s, 2H), 7.23-7.21 (m, 2H)

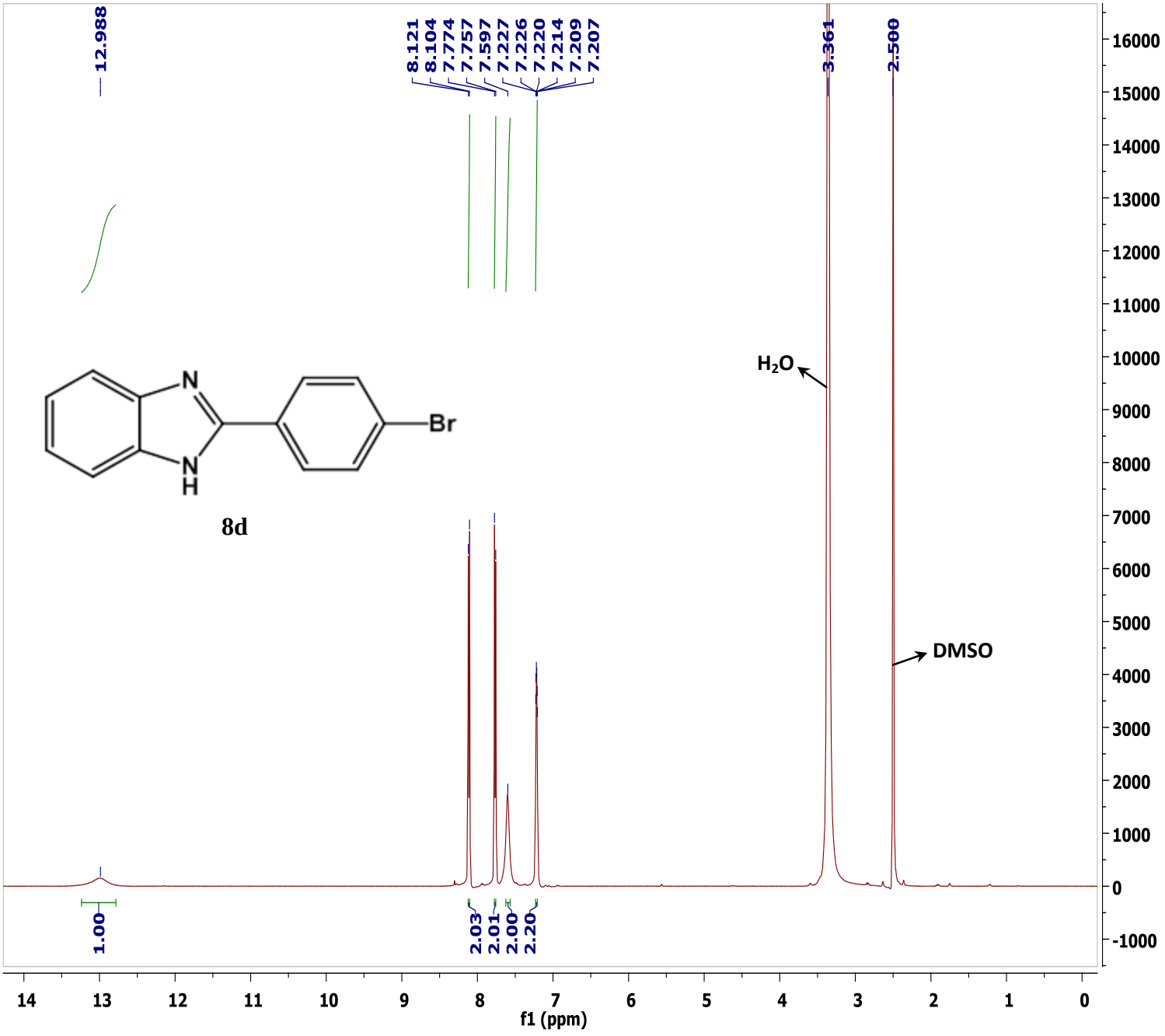

Figure S37 ^{1}H NMR spectrum of compound **8d**

Compound 8e[8] White solid; 2-(4-chlorophenyl)-1*H*-benzo[d]imidazole: (0.150 g in 61% yield). ^{1}H NMR (500 MHz, DMSO-d_6, ppm) δ 12.98 (br s, 1H), 8.18 (d, *J* = 8.5 Hz, 2H), 7.63 (d, *J* = 8.5 Hz, 3H), 7.54 (s, 1H), 7.22 (s, 2H)

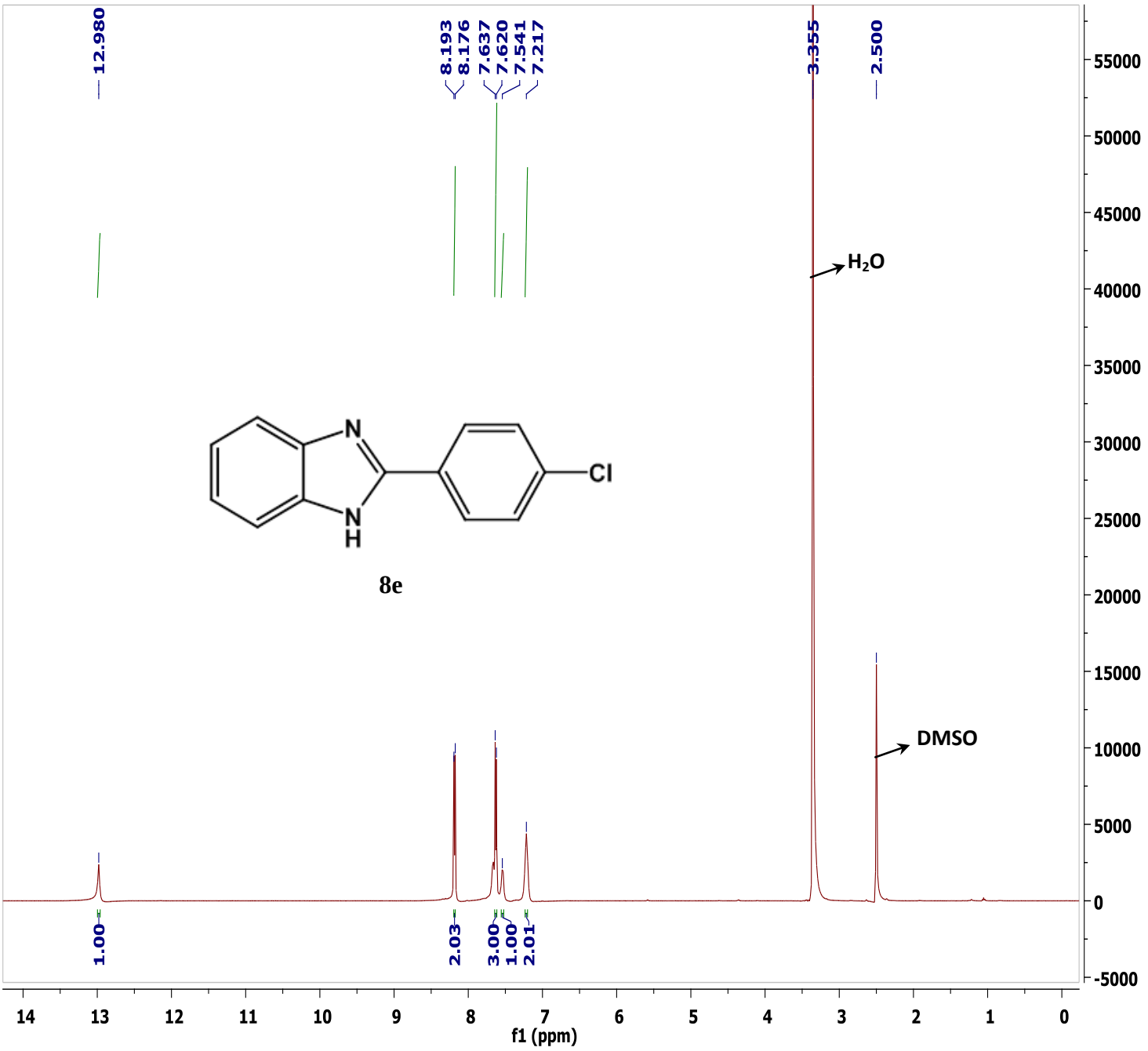

Figure S38 ^{1}H NMR spectrum of compound **8e**

Compound 8f[7,8] Yellow solid; 2-(4-nitrophenyl)-1*H*-benzo[d]imidazole: (0.157 g in 61% yield). ^{1}H NMR (500 MHz, DMSO-d_6, ppm) δ 13.28 (br s, 1H), 8.42 (s, 4H), 7.72 (s, 1H), 7.61 (s, 1H), 7.27 (s, 2H)

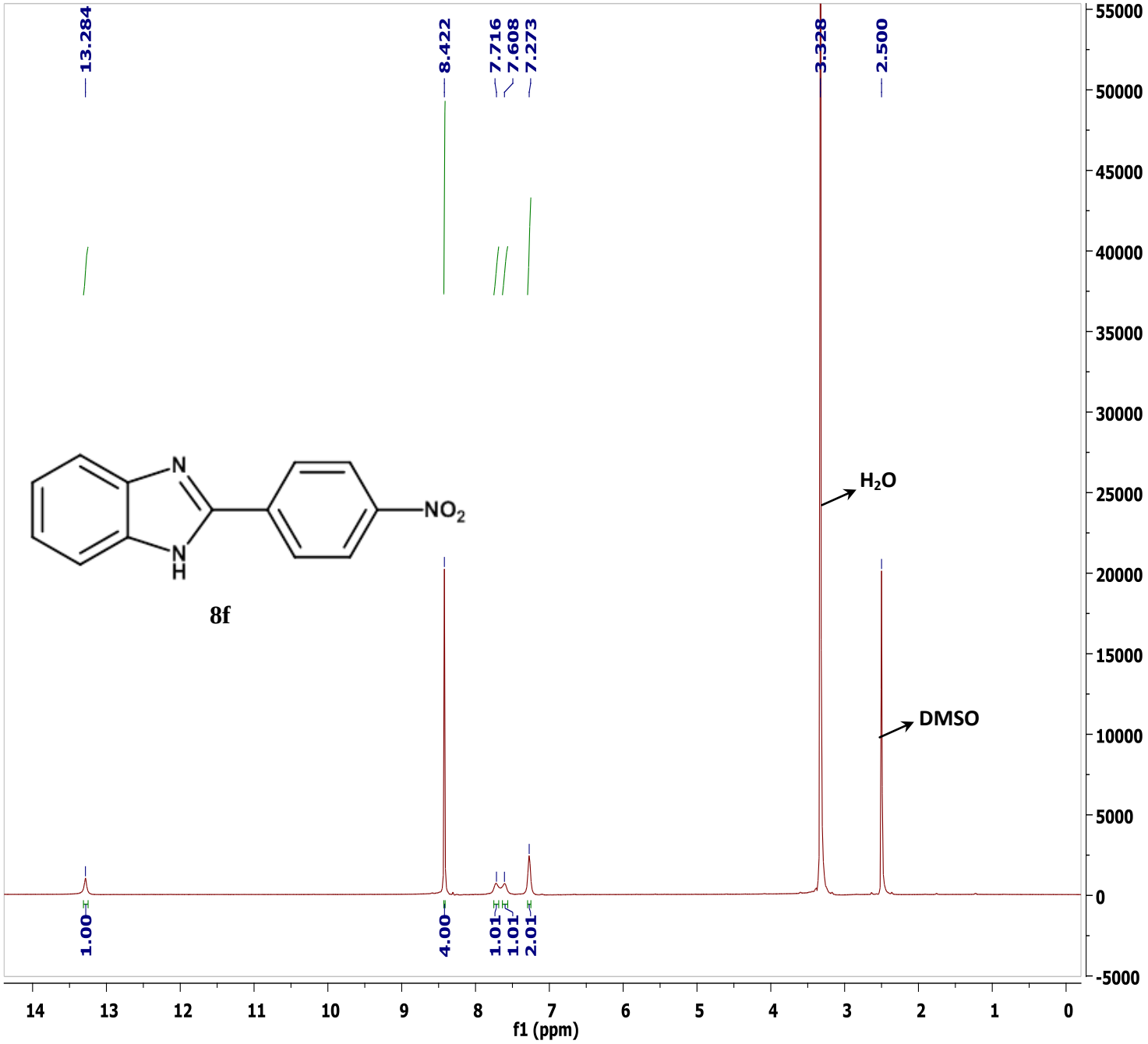

Figure S39 ^{1}H NMR spectrum of compound **8f**

Compound 8g[9,10] White solid; 2-(m-tolyl)-1*H*-benzo[d]imidazole: (0.170 g in 76% yield). ^{1}H NMR (500 MHz, DMSO-d_6, ppm) δ 12.84 (s, 1H), 8.02 (s, 1H), 7.96 (d, *J* = 7.5 Hz, 1H), 7.65-7.51 (m, 2H), 7.43 (t, *J* = 7.5 Hz, 1H), 7.31 (d, *J* = 7.5 Hz, 1H), 7.21-7.18 (m, 2H), 2.42 (s, 3H).

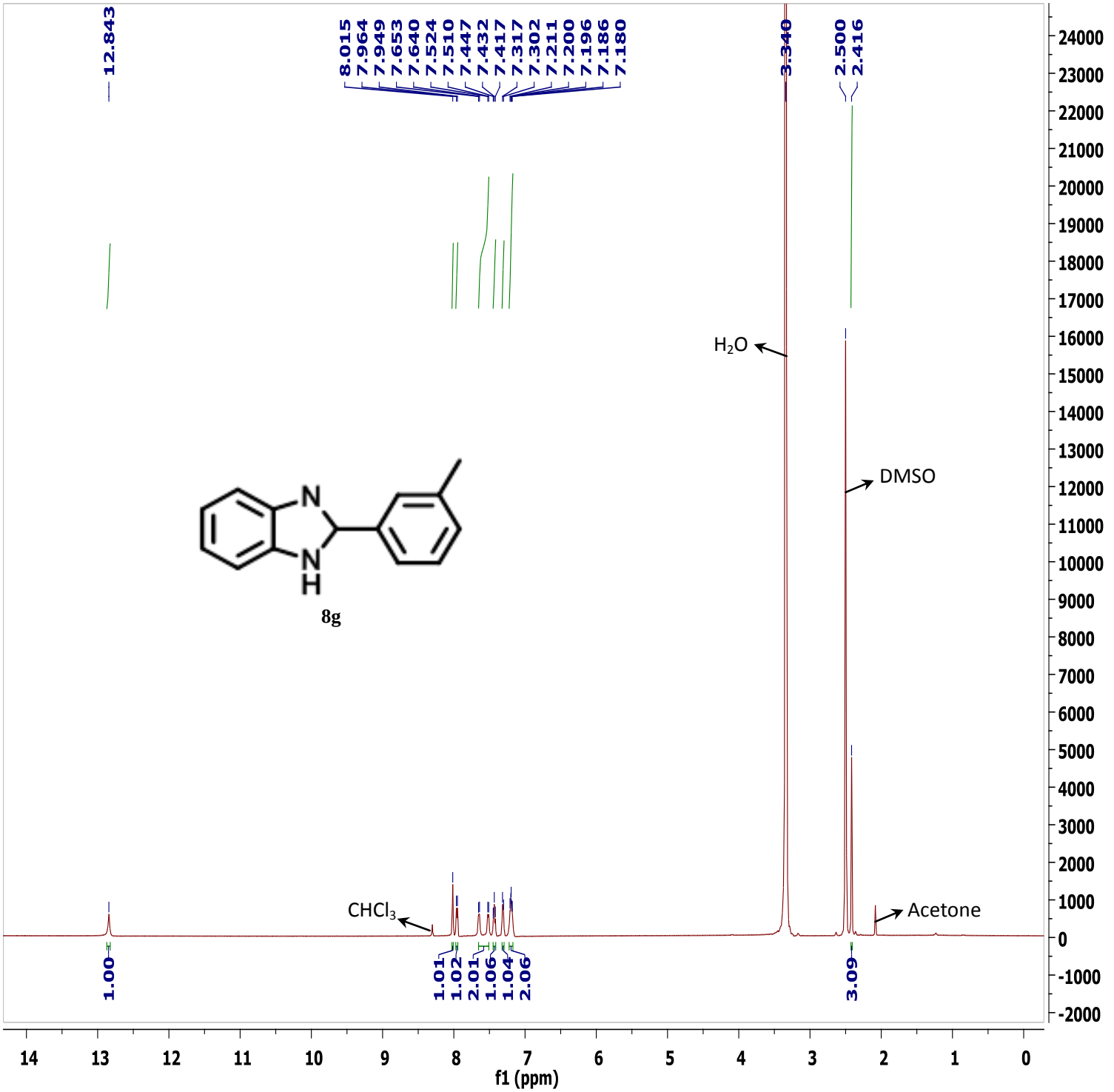

Figure S40 ^{1}H NMR spectrum of compound **8g**

Compound 8h[10] White solid; 2-(o-tolyl)-1*H*-benzo[d]imidazole: (0.165 g in 74% yield).[1]H NMR (500 MHz, DMSO-d_6, ppm) δ 12.59 (s, 1H), 7.73 (d, *J* = 7.5 Hz, 1H), 7.67 (d, *J* = 7.5 Hz, 1H), 7.52 (d, *J* = 7.5 Hz, 1H), 7.39-7.35 (m, 3H), 7.24-7.17 (m, 2H), 2.60 (s, 3H).

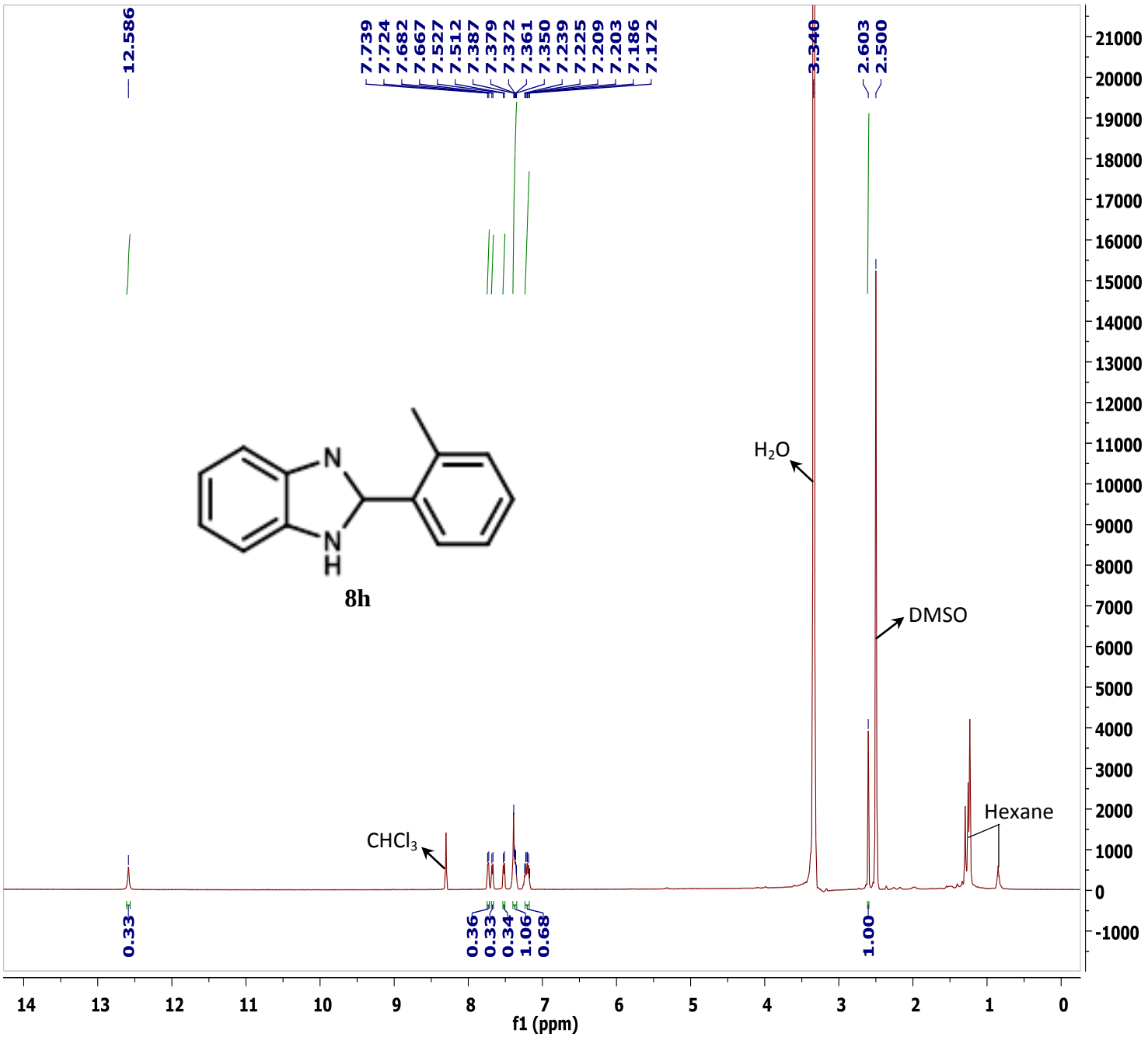

Figure S41 [1]H NMR spectrum of compound **8h**

Compound 8i[8] White solid; 2-(3,5-Dimethylphenyl)-1*H*-benzo[d]imidazole: (0.200 g in 84% yield).[1]H NMR (500 MHz, DMSO-d_6, ppm) δ 12.80 (br s, 1H), 7.80 (s, 2H), 7.63 (s, 1H), 7.50 (s, 1H), 7.19 (s, 2H), 7.13 (s, 1H), 2.37 (s, 6H)

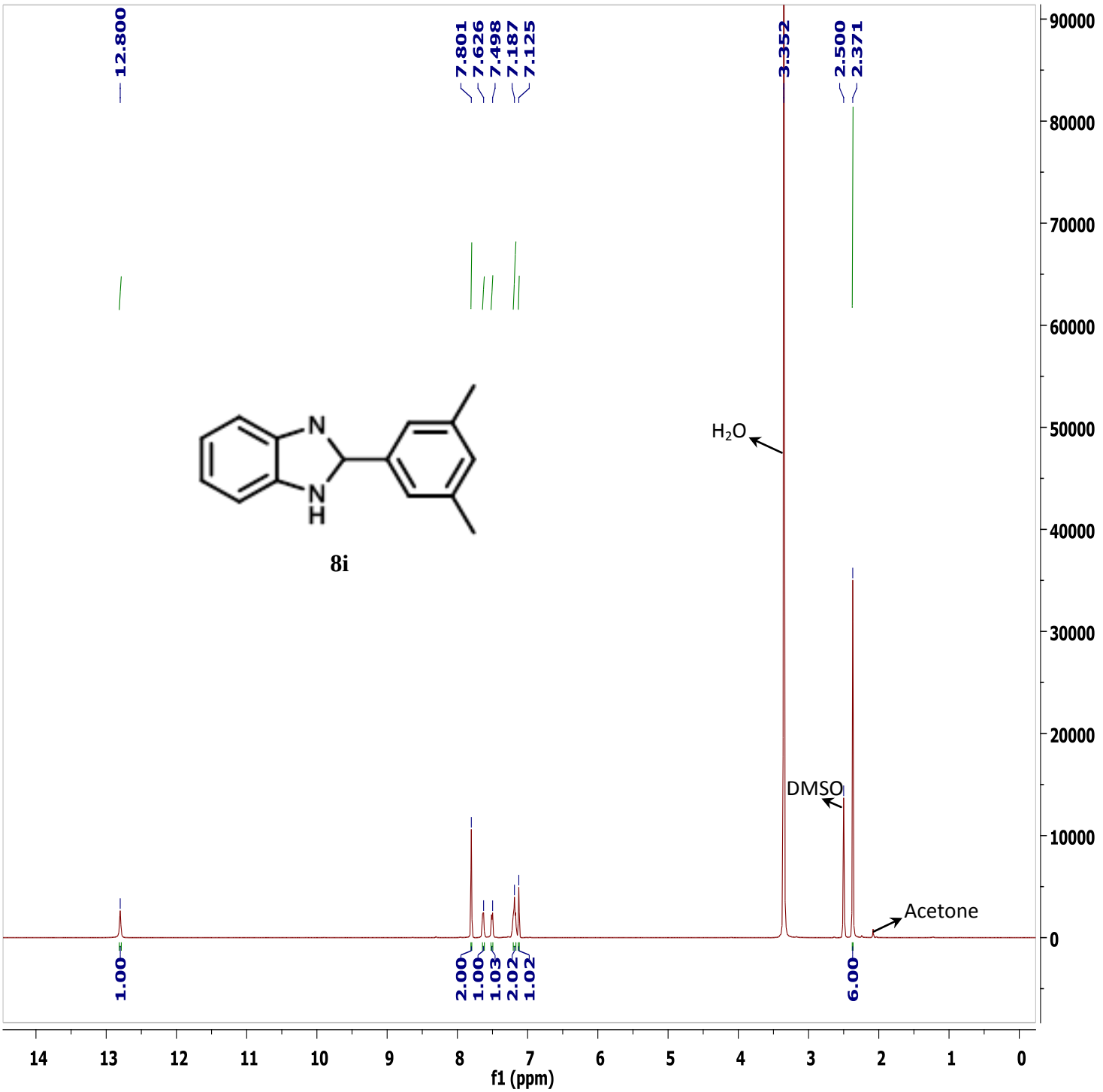

Figure S42 [1]H NMR spectrum of compound **8i**

Compound 8j[8] White solid; 6-Bromo-2-(3,5-dimethylphenyl)-1*H*-benzo[d]imidazole: (0.122 g in 70% yield). ^{1}H NMR (500 MHz, DMSO-d_6, ppm) δ 13.02 (br s, 1H), 7.79 (s, 2H), 7.66-7.47 (m, 2H), 7.33 (s, 1H), 7.15 (s, 1H), 2.37 (s, 6H)

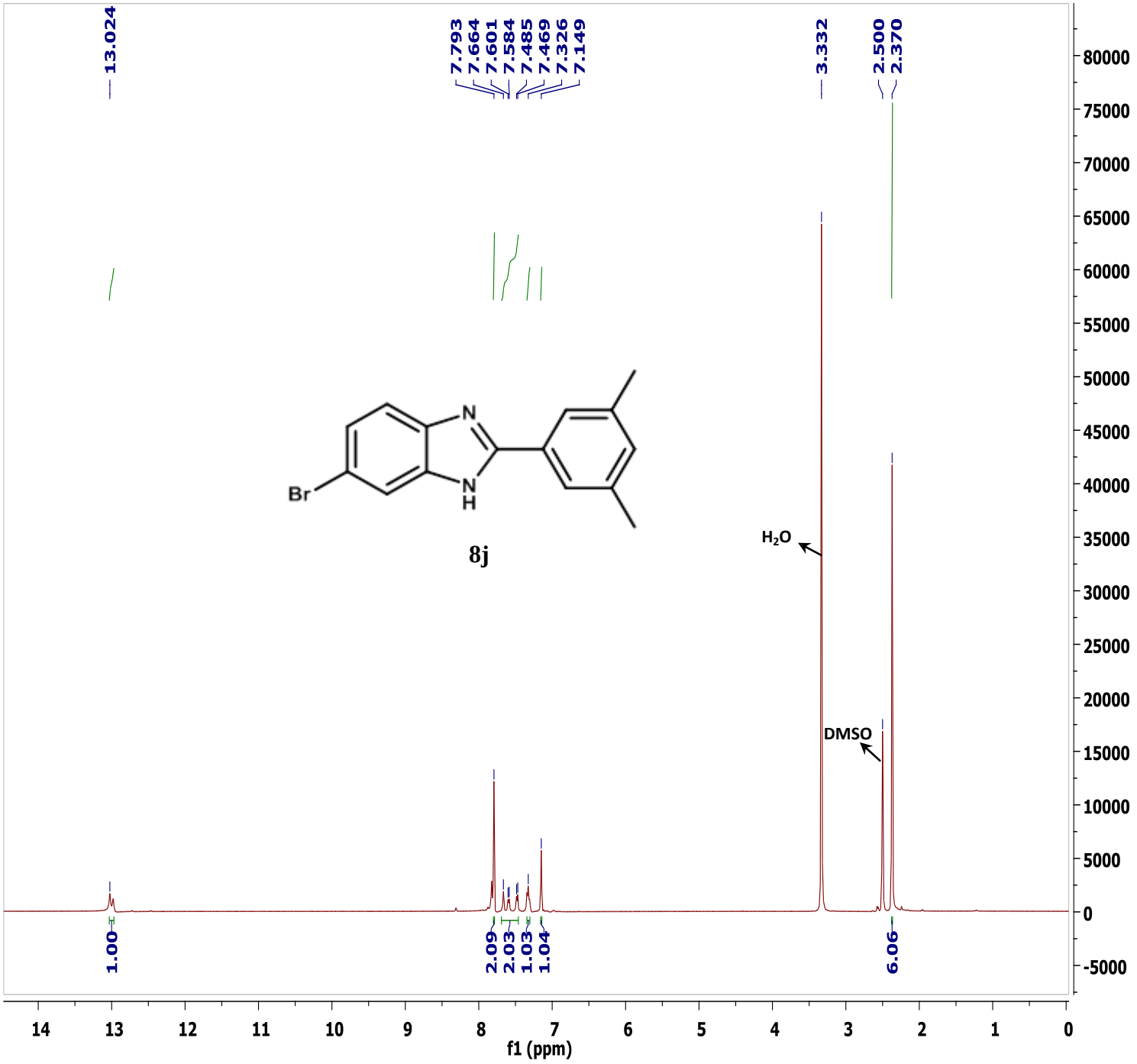

Figure S43 ^{1}H NMR spectrum of compound **8j**

Compound 8k[8] White solid; 6-Chloro-2-(3,5-dimethylphenyl)-1*H*-benzo[d]imidazole: (0.131 g in 65% yield). ^{1}H NMR (500 MHz, DMSO-d_6, ppm) δ 13.02 (br s, 1H), 7.79 (s, 2H), 7.68-7.63 (m, 1H), 7.53 (s, 1H), 7.22 (d, *J* = 5.5 Hz, 1H), 7.15 (s, 1H), 2.37 (s, 6H)

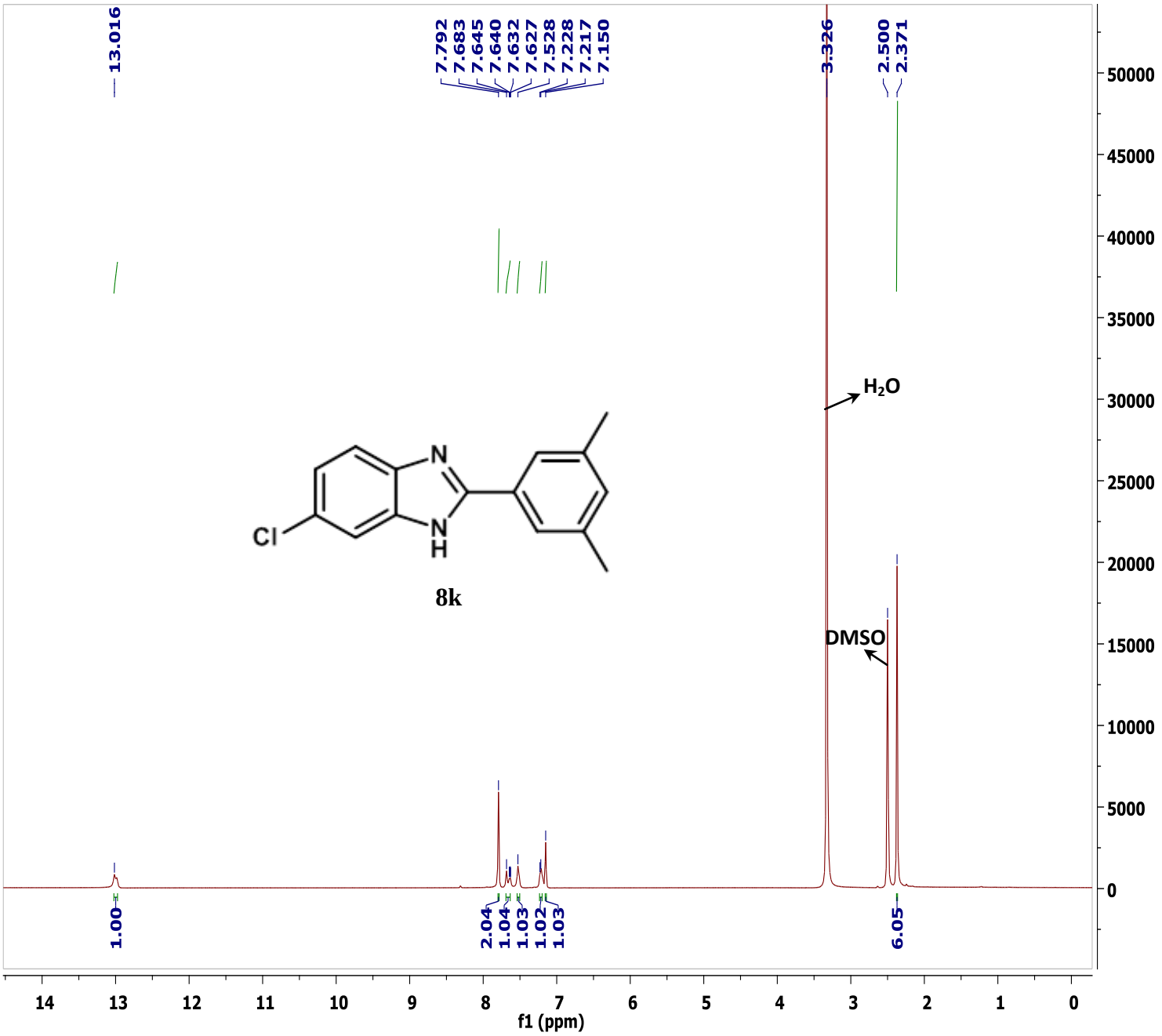

Figure S44 ^{1}H NMR spectrum of compound **8k**

Compound 8m[8] White solid; 2-(3,5-Dimethylphenyl)-4-methyl-1*H*-benzo[d]imidazole: (0.181 g in 82% yield). mixture of tautomers (1:1); ^{1}H NMR (500 MHz, DMSO-d_6, ppm) δ 12.73 (br s, 1H), 12.48 (br s, 1H), 7.86 (s, 2H), 7.79 (s, 2H), 7.44 (d, *J* = 8.0 Hz, 1H), 7.31 (d, *J* = 8.0 Hz, 1H), 7.12-7.07 (m, 4H), 6.99-6.96 (m, 2H), 2.57 (s, 3H), 2.55 (s, 3H), 2.37 (s, 12H)

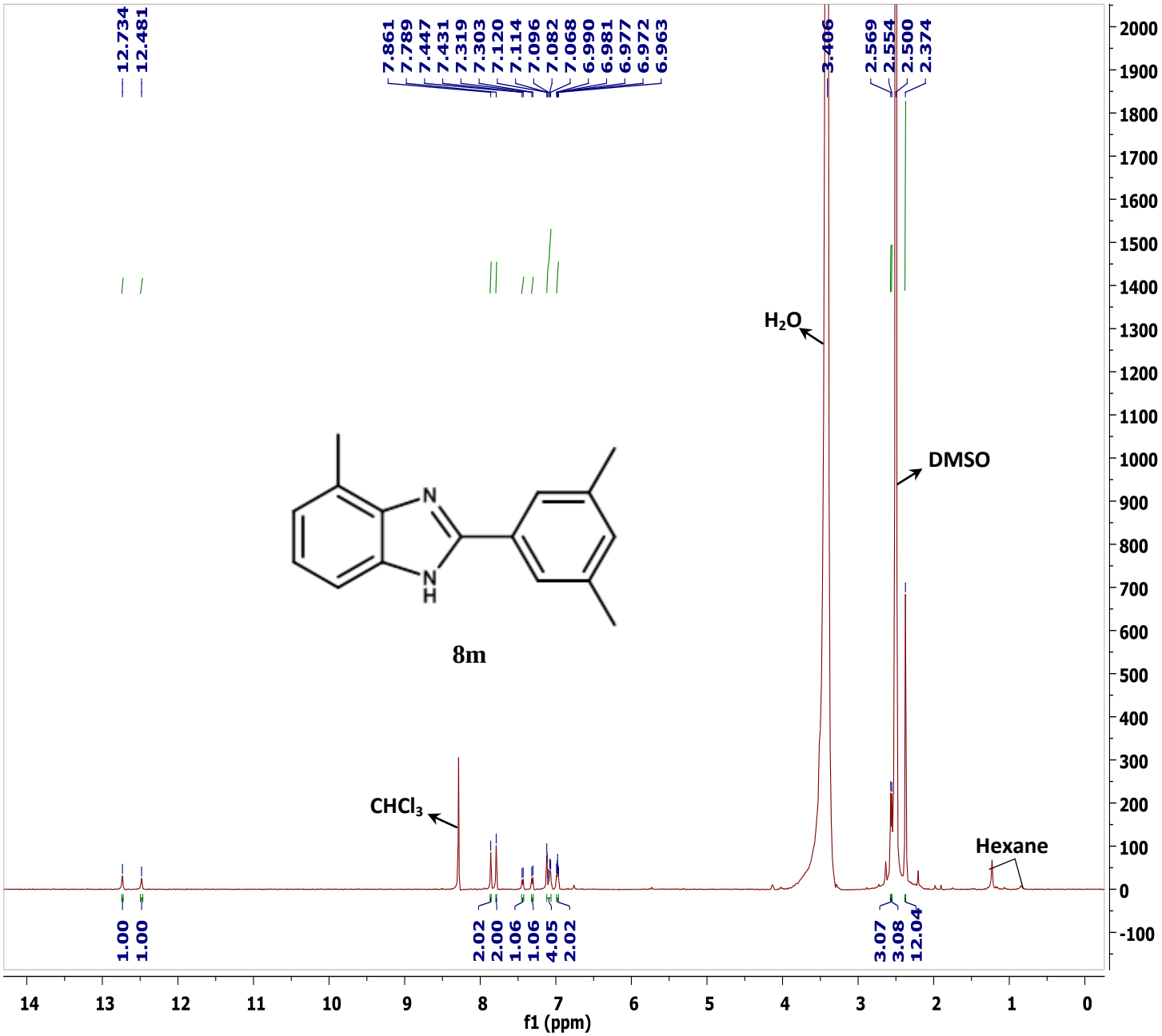

Figure S45 ^{1}H NMR spectrum of compound **8m**

Compound 8n[8] White solid; 2-(3,5-Dimethylphenyl)-4,7-dimethyl-1*H*-benzo[d]imidazole: (0.180 g in 87% yield). ^{1}H NMR (500 MHz, DMSO-d_6, ppm) δ 12.40 (br s, 1H), 7.88 (s, 2H), 7.12 (s, 1H), 6.87 (s, 2H), 2.53-2.51 (m, 6H), 2.39 (s, 6H)

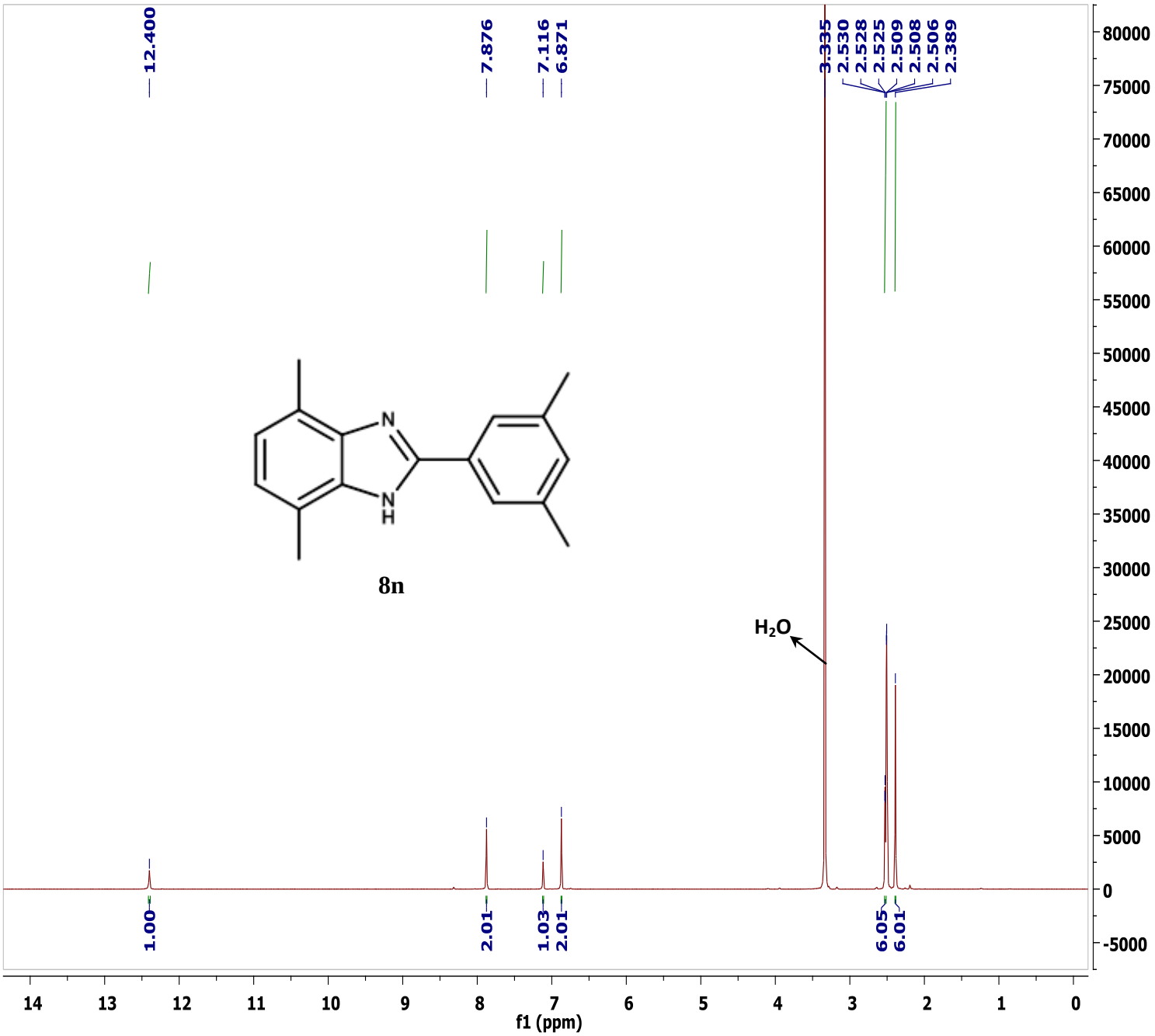

Figure S46 ^{1}H NMR spectrum of compound **8n**

Compound 4 Orange solid; (0.294 g in 56% yield) ^{1}H NMR (400 MHz, $CDCl_3$, ppm) δ = 8.94 (s, 2H), 8.93 (s, 2H), 8.23 (s, 2H), 8.14 (d, *J* = 8.8 Hz, 2H), 7.94 (d, *J* = 8.8 Hz, 2H), 7.74 (d, *J* = 8.8 Hz, 2H), 7.61 (d, *J* = 8.8 Hz, 2H), 7.53 (d, *J* = 8.8 Hz, 2H), 6.84 (d, *J* = 8.8 Hz, 2H)

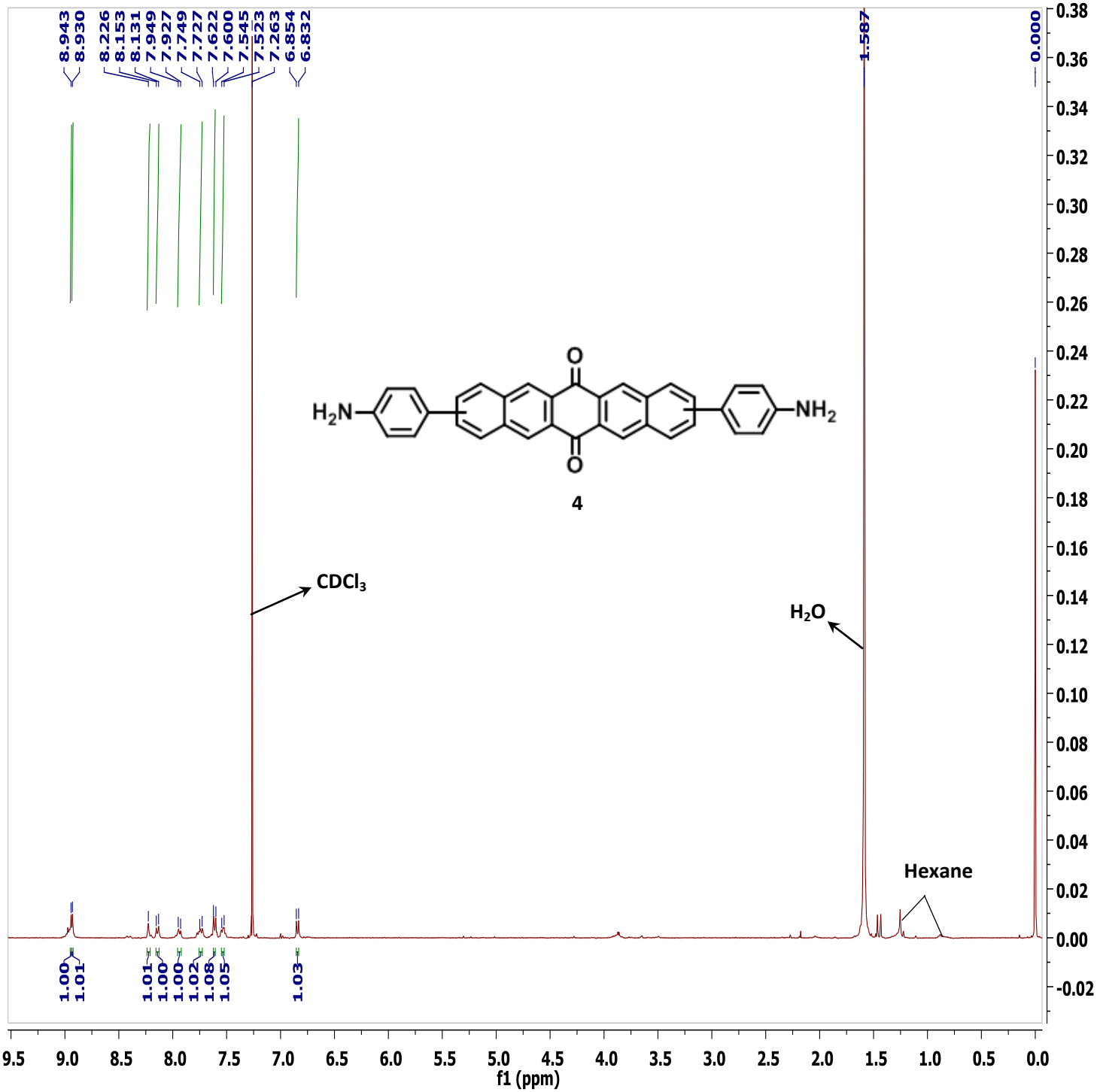

Figure S47 ^{1}H NMR spectrum of compound **4**

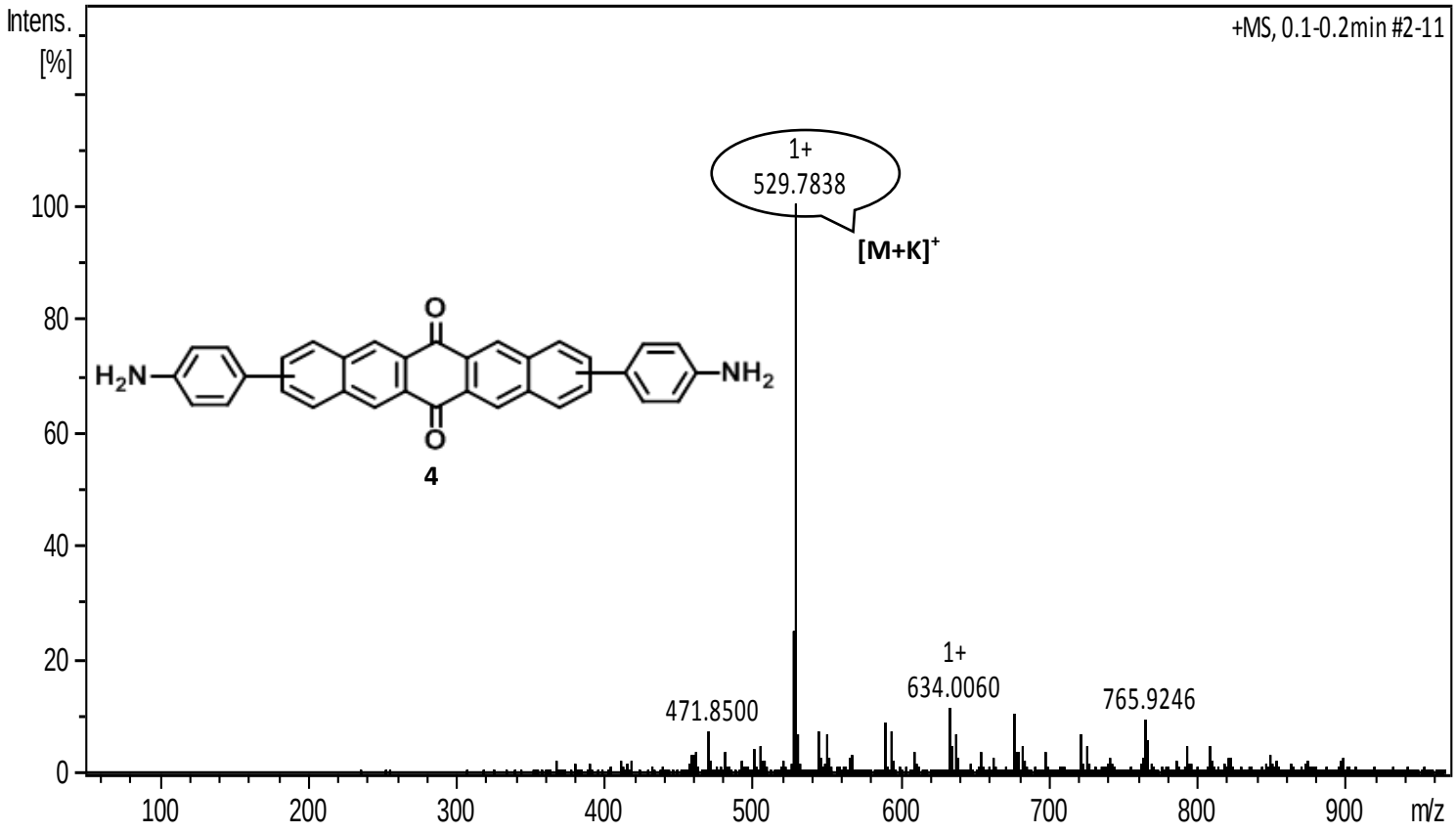

Figure S48 Mass spectrum of compound **4**.

REFERENCES:

(1) R. Chopra, M. Kumar and V. Bhalla, *ACS Sustainable Chem. Eng.*, 2018, **6**, 7412-7419.

(2) M. L. Błocho, K. Pacławski, M. Wojnicki and K. Fitzner, *Inorganica Chimica Acta*, 2013, **395**, 189-196.

(3) T. K. Sau and C. J. Murphy, *Langmuir*, 2004, **20**, 6414-6420; (b) S. Goswami, S. Das, K. Aich, D. Sarkar, T. K. Mondal, C. K. Quah and H. K. Fun, *Dalton Trans.*, 2013, **42**, 15113-15119.

(4) J. He, L. Chen, D. Ding, Y. K. Yang, C. T. Au, S. F. Yin, *Appl. Catal. B: Environ.* 2018, **233**, 243-249.

(5) C. Meng, K. Yang, X. Fu, R. Yuan, *ACS Catal.*, 2015, **5**, 3760.

(6) (a) T. M. Brown, C. J. Cooksey, D. Crich, A. T. Dronsfield and R. Ellis, *J. Chem. Soc., Perkin Trans*, 1993, **1**, 2131-2136; (b) T. W. Liwosz and S. R. Chemler, *Org.Lett.*, 2013, **15**, 3034-3037.

(7) A. Kasprzak, M. Bystrzejewski and M. Poplawska, *Dalton Trans.*, 2018, **47**, 6314-6322.

(8) D. Mahesh, V. Satheesh, S. V. Kumar and T. Punniyamurthy, *Org. Lett.*, 2017, **19**, 6554-6557.

(9) L. Li, Q. Luo, H. Cui, R. Li, J. Zhang and T. Peng, *ChemCatChem*, 2018, **10**, 1607-1613.

(10) R. Zhang, Y. Qin, L. Zhang and S. Luo, *Org. Lett.*, 2017, **19**, 5629-5632.